Catalysis Letters (2021) 151:3343–3360
https://doi.org/10.1007/s10562-021-03575-y

Converting Cyclohexanone to Liquid Fuel-Grade Products: A Characterization and Comparison Study of Hydrotreating Molybdenum Catalysts

Ali Bakhtyari[1] · Adele Sakhayi[1] · Zohre Moravvej[1] · Mohammad Reza Rahimpour[1]

Received: 21 November 2020 / Accepted: 15 February 2021 / Published online: 4 March 2021

Abstract

Developing biomass-based strategies for liquid bio-fuels production is promising for the reduction of the aftereffects of fossil fuels. The conversion of lignin-derived intermediates such as cyclohexanone is currently of a great deal of interest. The current study aims to evaluate the molybdenum-based hydrotreating catalysts for the conversion of cyclohexanone in the presence of hydrogen. Catalytic experiments at 400 °C, 15 bar, and a range of WHSV were developed. The experiments reveal that catalyst type and reaction WHSV affect the cyclohexanone conversion, product distribution, deoxygenation efficiency, total hydrocarbon production capacity, and heating value of the product blend. The main products include C_6 cyclic and aromatic hydrocarbons and oxygenates. Cyclohexane, cyclohexene, benzene, cyclohexanol, and phenol are major products. Small quantities of methylcyclopentane and bicyclic hydrocarbons and oxygenates are also reported in some cases. Increasing WHSV reduced the cyclohexanone conversion. Cyclohexanone conversions up to 89% were observed at the lowest WHSVs over a cobalt-molybdenum sample. The highest hydrocarbon production capacity (99.53%) was managed at WHSV = 5.240 $g_{cyclohexanone}/g_{cat}$ h over a cobalt-molybdenum sample, while the highest deoxygenation efficiency, i.e. 81.29% degree of deoxygenation and 5.35 C/O ratio enhancement were achieved at WHSV = 0.262 $g_{cyclohexanone}/g_{cat}$ h by a nickel-molybdenum sample. The heating values would be enhanced by up to 22.7% when cyclohexanone is converted over the utilized catalysts. The larger heating value (44.90 MJ/kg, 22.7% enhancement) was obtained over a nickel-molybdenum catalyst, which is comparable to the energy density of the conventional fuels. The results reveal that the catalysts are efficient in the conversion of cyclohexanone to liquid bio-fuels.

Graphic Abstract

Keywords Bio-fuel · Hydrodeoxygenation · Cyclohexene · Cyclohexane · Heating value · Hydrocarbon

Extended author information available on the last page of the article

1 Introduction

Over the past few years, the utilization of nonrenewable resources such as fossil hydrocarbons has been considered a global concern. The reduction of fossil sources, ascending global demand for energy carriers and chemicals, environmental defects, and climate change have caused such a concern [1–4]. In this regard, significant efforts for the production of energy carriers, as well as chemicals, from sustainable and renewable sources have been gaining momentum [4–8]. The main avenues to succeed in producing renewable and sustainable fuels and chemicals are based on the utilization of biomass. Biomass is an outstanding alternative owing to its carbon neutrality, wide availability, and low cost [5, 7–12]. The conversion of lignocellulosic biomass is currently a major trend. Lignocellulose is the most abundant non-edible biomass source with high potential to produce various biocompatible liquid fuels and chemicals [4, 13, 14]. Pyrolysis is an efficient process to obtain bio-oil through the conversion of lignocellulosic components, i.e. cellulose, hemicellulose, and lignin [12, 15, 16]. Lignin is made up of aromatic components and is a promising source for the production of liquid fuels and chemicals [4, 17–21]. However, the bio-oil derived from lignin is unstable, acidic, and rich in oxygenated compounds with a low thermal value (approximately half the value of fossil fuels) [2, 3, 22–24]. Hence, gasoline-type and jet-fuel range liquids, as well as the octane boosters, can be produced through the upgrading of the lignin-derived bio-oils [23, 25–29]. To do so, hydrodeoxygenation (HDO) by employing metal-based acidic catalysts under the hydrogen atmosphere is currently an effective process [2, 3, 30–32]. Significant efforts have been devoted to evaluating highly active and selective catalysts for upgrading the lignin-derived model compounds to hydrocarbon liquid fuels. The catalysts that are made up of noble metals (such as palladium, platinum, and ruthenium) and non-noble metals (such as nickel, cobalt, and molybdenum) are various types of catalysts that were employed for the HDO process. Lignin-derived compounds bearing hydroxyl and/or methoxy oxygen functional groups such as phenols, anisoles, and guaiacols, eugenols, and vanillyl alcohol are well investigated in the previous studies [3, 33, 34]. Lignin-derived bio-oils, as well as the major portion of the products of the HDO of phenols, anisoles, and guaiacols, include ketonic (C = O) functional group [2, 3, 35, 36]. The products of the process contain also the saturated ring and C = O functional group. The HDO of cyclic compounds incorporating ketonic oxygen groups such as cyclohexanone [37–43] is not well investigated. Hence, the HDO of cyclohexanone to produce fuel-range products is currently state of the art.

In this regard, the HDO of cyclohexanone was investigated on Pt/HZSM-5 catalysts by Alvarez et al. [44]. The main observed products included six-carbon cyclic hydrocarbons, twelve-carbon bicyclic hydrocarbons, and tricyclic ketones. Comprehensive reaction schemes were also proposed for the formation of such products [44]. The conversion of cyclohexanone to cyclohexylcyclohexanone on Pd/faujasite catalysts was investigated by Silva et al. [45]. They reported aldolisation, dehydration, and hydrogenation reactions when the synergy of metallic (0.1–0.5 wt. % of Pd) and acid functions (Si/Al ratio of 5–100) was evaluated. Utilizing the unsupported Ni-W sulfided catalysts in the HDO of cyclohexanone led to the formation of cyclohexene with high selectivity [46]. Based on the observations of Nimmanwudipong et al. [37], the HDO of cyclohexanone on Pt/γ-Al_2O_3 catalyst proceeds toward the generation of mono/bicyclic hydrocarbons as well as the oxygenated bicyclics. Accordingly, a complex reaction path including hydrogenation/dehydrogenation, dehydration, isomerization/alkylation, and aldol condensation is responsible for the conversion of cyclohexanone to such classes of products on Pt/γ-Al_2O_3 catalyst. In a further study from this research group, Runnebaum et al. [38] classified the reactions that are responsible for oxygen removal and those that resulted in the formation of oxygenated compounds. The products of these two groups included six-carbon cyclic hydrocarbons (benzene, cyclohexane, and cyclohexene) and oxygenates (cyclohexanol, cyclohexenone, and phenol), respectively. Based on the observations of Prasomsri et al. [47], molybdenum trioxide, i.e. MoO_3 was an efficient catalyst for the hydrogenolysis of the carbonyl group and further production of cyclohexene, benzene, and biphenyl. Kong and colleagues [48–50] examined the capability of ZSM-based Ni catalysts for the HDO of cyclohexanone. They also investigated the effect of alkali-treating and the type and composition of binder on the performance of the catalysts. The well-dispersed Ni particles, well-defined mesoporosity, and proper proceeding of the reaction path toward the desired products were achieved by adjusting these parameters. The kinetic study of the HDO of cyclohexanone at the low conversions on Pt/γ-Al_2O_3 catalyst was conducted by Saidi et al. [39]. Their results indicated that the reaction system includes hydrogenation, dehydrogenation, hydrodeoxygenation, dehydration, and condensation. They employed pseudo-first-order rate expressions to the collected experimental data. A similar study was then conducted by utilizing the sulfided cobalt-molybdenum (CoMo) catalyst by Saidi and Jahangiri [26].

Despite the fact that some synthetic and commercial catalysts have been hitherto evaluated for the HDO of cyclohexanone, there is still room for improvement and investigation of this process. To do so, the catalysts based

on molybdenum and promoted by nickel (NiMo) and cobalt (CoMo) are of great commercial interest. These catalysts are well-considered for the hydrotreating reactions and upgrading of other lignin-derived compounds [51–60]. As far as the authors know, the lack of a rigorous comparison to select an optimum commercial hydrotreating catalyst for the conversion of cyclohexanone to fuel-range products is still felt. Accordingly, the present contribution aims to characterize and compare the conventional alumina-supported hydrotreating NiMo and CoMo catalysts for the conversion of cyclohexanone to fuel-range products. The experiments at mild reaction temperature and pressure, which correspond to higher conversion and product yield, and a range of reactant to catalyst ratio, are conducted.

2 Experimental

2.1 Catalyst Characterizations

The provided catalysts, as well as their suppliers and appearance, are summarized in Table S1 in the Supporting Information. To determine the active phases, acidity, particle dispersion, and textural properties of the catalyst samples, characterization techniques including X-ray diffraction (XRD), temperature-programmed reduction of hydrogen (H_2-TPR), temperature-programmed desorption of ammonia (NH_3-TPD), energy-dispersive X-ray spectroscopy (EDXS), and N_2 adsorption and desorption were employed.

A Bruker D8 Advance powder X-ray diffractometer with a Cu-Kα monochromatizer (40 kV, 40 mA) was employed to extract the XRD of $2\theta = 5°–80°$ with 0.02° step sizes. The H_2-TPR spectra and the reduction states of the samples were determined by employing NanoSORD NS91 (Sensiran). The experiment included sample weighting (~ 50 mg), placing in the U-shaped reactor, heating up to 300 °C (10 ml/min) by helium steam, degassing, cooling to room temperature, and heating (10 °C/min) up to 900 °C by a hydrogen-containing stream (10 ml/min, 5% H_2, 95% Ar). The output stream was then analyzed by a thermal conductivity detector (TCD). NH_3-TPD spectra and the acidity of the samples were determined by the same apparatus. The experiments included a degassing procedure similar to that of the H_2-TPR experiment, saturating by NH_3 (5%) at 120 °C, and heating up to 750 °C (10 °C/min) by pure helium stream. The output stream was then analyzed by the TCD. Metal dispersion was scanned by TESCAN-Vega 3 with a 5 kV accelerating voltage. ASAP-2020 of Micromeritics was employed to collect N_2 adsorption and desorption isotherms at 77 K. The range of measurements includes $p/p_0 = 0.001–0.999$. To determine surface area, pore volume, and pore size distribution, the well-known Brunauer–Emmett–Teller (BET), Langmuir, t-plot, and Barret-Joyner-Halenda (BJH) methods were employed.

2.2 Catalytic HDO of Cyclohexanone

The utilized reaction system for the catalytic HDO experiments was Microactivity-reference, PID Eng & Tech. The apparatus and the experimental procedure is well introduced in the previously published works [39, 41, 51, 52, 61–65]. In summary, the apparatus involves an upstream pre-evaporator, mixing chamber, a one-way stainless-steel tube (30.5 cm length and 0.9 cm diameter) employed as the fixed catalyst bed, an electric heating jacket, a downstream catalyst fines filter (10 µm), a pressure transducer, and control valve. The instruments are located in a box that is heated by a forced convection heater. Hence, the condensation of vapor-containing streams in the lines is prevented.

The typical experiments included weighting catalyst and loading in the tube, the pressurizing system to 15 bar total pressure with hydrogen (99.999%), heating to the reduction temperature (400 °C), 1 h in-situ catalyst reduction under hydrogen stream (6 L/h), and injection of the reactant mixture (3 wt.% cyclohexanone, 0.97 wt.% n-decane) with the desired flow rate (~ 0.1 mL/min) by a Gilson, 307 HPLC pump. The injected reactant mixture was then evaporated and blended with the hydrogen stream and was then sent to the catalyst fixed-bed. The discharged stream was then cooled by employing a counter-current condenser (− 2–0 °C) and the condensed liquid collected (2 h) for the analysis. More details of the experimental procedure could be found elsewhere [40–42]. The weight hourly space velocity (WHSV) was determined by adjusting the reactant mixture flowrate and catalyst weight. Hence, the WHSV and hydrogen-to-cyclohexanone molar ratios were 0.262–5.389 $g_{cyclohexanone}/g_{cat}$ h and ~ 1400, respectively.

The collected product was analyzed qualitatively and quantitatively by a gas chromatograph-mass spectrometer (GC–MS, Agilent 7890B) equipped with an HP-5 ms capillary column. More details of the analysis procedure could be found elsewhere [40–42]. The conversion of cyclohexanone, product selectivity, product yield, the degree of deoxygenation (DDO%), and C/O Ratio Enhancement (C/O RE) are determined by Equations S1–S5 [66–70] of the Supporting Information. Furthermore, to assess the capability of the final blend as a potential fuel, higher heating values (HHV) of the lignocellulosic materials are estimated by Equation S6 [71]. Lower heating values (LHV) are then estimated by Equation S7 [72]. In Equations S1–S7, n and wt denote the number of moles and weight percent, respectively.

3 Results and Discussion

3.1 Catalyst Characterizations

The results of EDXS elemental analysis, as well as elements distributions of the catalyst samples, are tabulated in Table 1. It is worth mentioning that each reported quantity is the average of 3 consecutive scans of three different areas. The distributions of the elements are also presented in Figures S1–S4 in the Supporting Information. As summarized in Table 1, the whole catalysts are molybdenum-based with smaller quantities of either cobalt or nickel as the promoter. The ratio of the promoter (either nickel or cobalt) to molybdenum is in the range of 0.080–0.208. Figures S1–S4 confirm that the whole particles are well distributed.

The XRD spectra of the alumina-supported CoMo and NiMo catalysts are depicted in Fig. 1. The wide peaks that are observed at 2θ ≈ 46°–47° and 2θ ≈ 67°–68° in the whole samples characterize the cubic aluminum oxide. The weak peaks that are observed at 2θ ≈ 44°, 52°, and 76° of CoMo samples characterize the cobalt oxides. The weak peaks of 2θ ≈ 38° and 65° of NiMo samples characterize the nickel oxides. The molybdenum oxides of CoMo samples are characterized by the observed peaks at 2θ ≈ 41°, 59°, and 74°. However, the peaks at ≈ 27°, 30°, 42°, 57°, and ≈ 75° in NiMo samples characterize the molybdenum oxides. Li et al. [73] reported that the observed peaks in the range of 2θ = 20°–35° of the CoMo catalyst are identified as $CoMoO_4$ crystallites. Similar observations were also reported by Van Venn et al. [74] and Jiang et al. [75]. It is also worth noting that the peaks of ≈ 27–28° of NiMo samples might be due to the formation of the β-$NiMoO_4$ phase. Such a behavior, on the other hand, occurs in the case of overloading nickel and molybdenum instead of their distinct monolayer dispersions. Such behavior was also reported and discussed in previous publications [76, 77]. Owing to the low concentration, well dispersion, and small size of cobalt and nickel particles, the weakly associated peaks were obtained. Such behavior was also reported in the previous studies dedicated to NiMo [78–81] and CoMo [82, 83] catalysts. The wt.%, as well as well particle distribution, were obtained by EDXS and mapping analysis (Table 1 and Figures S1–S4).

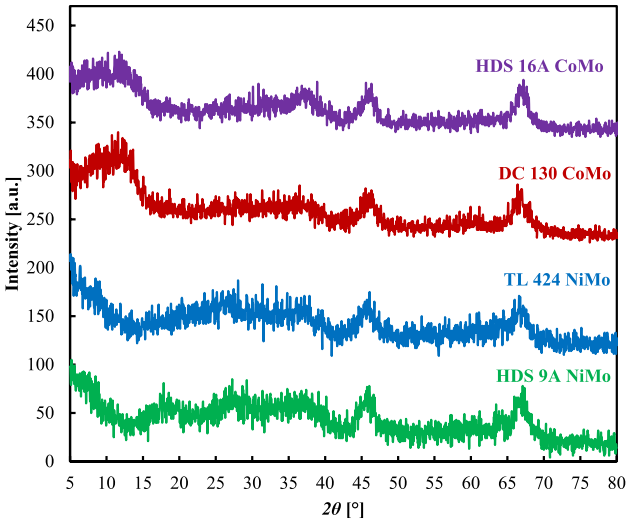

Fig. 1 XRD spectra of the examined hydrotreating catalysts

Figure 2 depicts the results of H_2-TPR experiments. Moreover, the obtained hydrogen uptakes are presented in Table 1. As per Fig. 2a, the sharp peaks observed at 300–600 °C are identified as Mo^{6+} to Mo^{4+} species that occur in amorphous multilayered molybdenum oxides or the dispersed octahedral polymeric structures made up of molybdenum [73, 84, 85]. Cordero et al. [84] reported that these structures often occur in the synthesis conditions of neutral pH. This peak is observed in all of the samples. It would be interesting to note that shifting this low-temperature peak to the higher temperatures in different samples attributed to the stronger interaction of molybdenum oxides with the support [73]. The second peak of CoMo samples at 550–670 °C is generally obtained as a result of the initial reduction of cobalt-molybdenum spinels of $CoMoO_4$ to $Co_2Mo_3O_8$ [73, 86]. The reduction of small quantities of the dispersed NiO species in NiMo catalysts is characterized by the small overlapped peaks obtained in the range of 520–690 °C. These particles are weakly bound to the surface of the alumina support [87, 88]. Further increase of

Table 1 Catalysts elemental composition, acidity, and H_2 uptake

Catalyst	Ni (wt.%)	Co (wt.%)	Mo (wt.%)	(Ni + Co)/Mo (–)	Al (wt.%)	O (wt.%)	Acidity (μmol $NH_3/g_{catalyst}$)	H_2 uptake (μmol/$g_{catalyst}$)
DC 130 CoMo	–	3.16	15.21	0.208	34.30	47.33	1207.7	2500.8
HDS 16A CoMo	–	2.33	12.49	0.187	33.46	51.72	1305.6	1804.6
TL 424 NiMo	1.14	–	14.27	0.080	26.05	58.54	1339.3	2261.1
HDS 9A NiMo	1.54	–	17.88	0.086	26.18	54.40	1966.6	2622.3

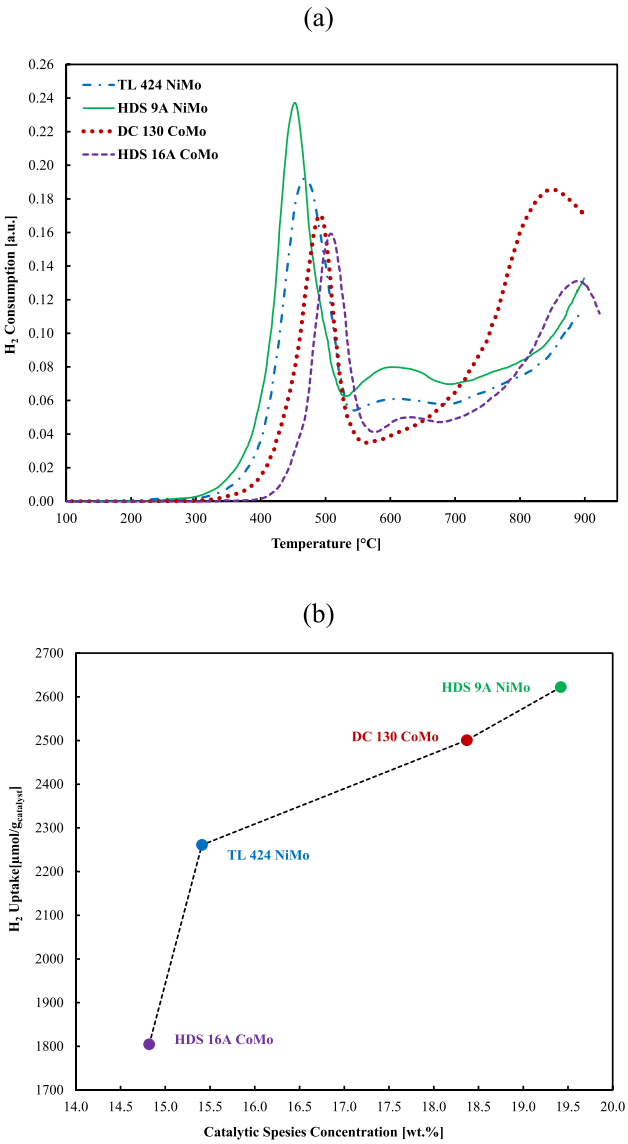

Fig. 2 H_2-TPR (**a**) and total hydrogen uptakes (**b**) spectra of the examined hydrotreating catalysts

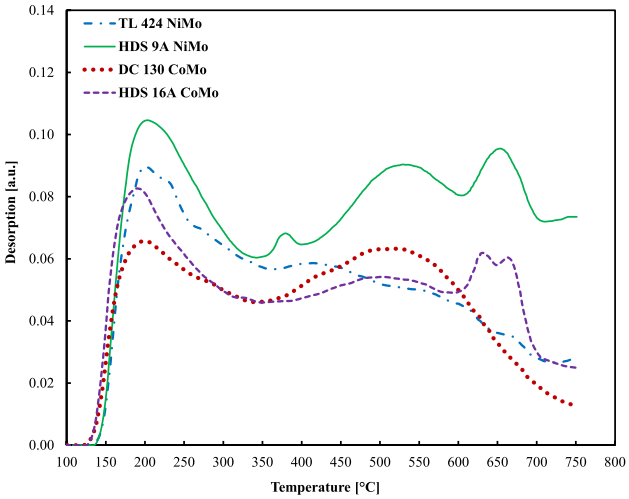

Fig. 3 NH_3-TPD spectra of the examined hydrotreating catalysts

temperature up to 900 °C results in the gradual and sharp increases in the hydrogen uptakes of NiMo and CoMo, respectively. The gradual increase of NiMo samples arises from the simultaneous reduction of Ni^{2+} species that exist in a spinel-type structure, deep reduction of the remaining molybdenum species, and the reduction of the tetrahedral molybdenum species that interact with alumina, strongly [84, 87, 89, 90]. The sharp increase of hydrogen uptake in the CoMo samples is also due to the total reduction of the whole remaining molybdenum species. This step involves a further reduction of as-reduced oxides at the lower temperatures as well as the initial reduction of the alumina-Mo^{6+} strongly bounded species [73, 85, 90]. The results of total hydrogen uptake that are depicted in Fig. 2b reveals that by increasing the total concentration of catalytic species, i.e. Ni + Co + Mo total hydrogen uptake increases. Larger quantities of hydrogen are on the one hand required to reduce the catalysts with larger concentrations of the catalytic species. In a practical point of view, the quantity of consumed hydroen in the catalyst pretreatement step is of process importance. The obtained hydrogen uptakes of HDS 16A CoMo, TL 424 NiMo, DC 130 CoMo, and HDS 9A NiMo catalyst are 1804.63 $\mu mol/g_{catalyst}$, 2261.13 $\mu mol/g_{catalyst}$, 2500.83 $\mu mol/g_{catalyst}$, and 2622.3 $\mu mol/g_{catalyst}$, respectively.

Figure 3 depicts the results of NH_3-TPD tests. The acidities of the samples in terms of ammonia desorption capacities are also tabulated in Table 1. As per Fig. 3, all of the samples are characterized by wide peaks at 150–350 °C, which attributes to the weak acidic sites [70, 91]. The spectra of TL 424 NiMo depict further gradual decay with increasing temperature, which confirms the heterogeneity of the strength of the acidic sites [80]. HDS 9A NiMo, HDS 16A CoMo, and DC 130 CoMo catalysts are furthermore characterized by the peaks at 450–700 °C. These peaks attribute to the medium-to-strong acidic sites [70, 91]. The HDS 9A NiMo sample exhibits a small peak at 350–400 °C, which is identified as medium acidic sites [70, 91]. There exist peaks (strong acidity) in the range of 650–700 °C in the spectra of the HDS samples. Alumina support produces acidity in the catalyst structure. Moreover, as reported by Damyanova et al. [92] and Laine et al. [93], the presence of Mo^{6+} species generates high acidity on the catalyst surface. As discussed earlier, the presence of Mo^{6+} species was confirmed by H_2-TPR experiments (Fig. 2). Hence, the differences in the NH_3-TPD patterns could be due to the different molybdenum and alumina concentrations (Table 1) [92, 93]. The acidities of DC 130 CoMo, HDS 16A CoMo, TL 424 NiMo, and HDS 9A NiMo samples in terms of ammonia desorption

capacity are 1207.7 μmol $NH_3/g_{catalyst}$, 1305.6 μmol $NH_3/g_{catalyst}$, 1339.3 μmol $NH_3/g_{catalyst}$, and 1966.6 μmol $NH_3/g_{catalyst}$, respectively. If we compare the compositions and acidities of HDS 9A and TL 424 NiMo catalysts, It is inferred that in almost constant nickel (1.14–1.54 wt.%) and aluminum (26.05–26.18 wt.%) contents, increasing molybdenum content (14.27–17.88 wt.%) resulted in the considerable acidity increase (2261.1–2622.3 μmol $NH_3/g_{catalysts}$). This reveals the role of molybdenum in the catalyst acidity.

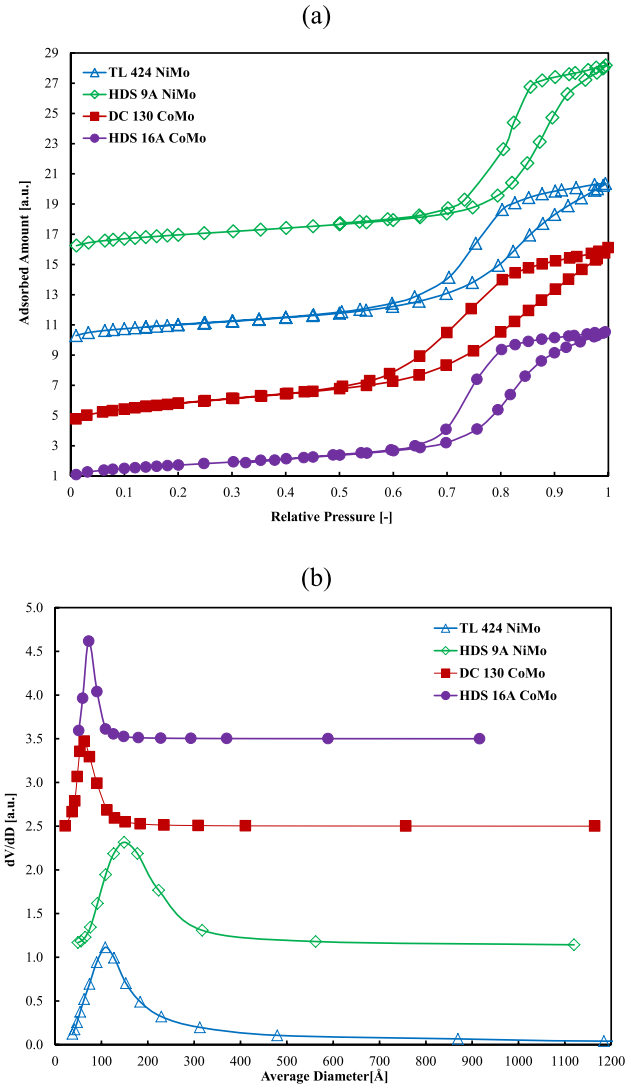

Fig. 4 Nitrogen adsorption/desorption isotherms (**a**) and pore size distributions (**b**) of the examined hydrotreating catalysts

Figure 4 depicts the collected adsorption/desorption isotherms of nitrogen at 77 K as well as the pore size distributions. As per Fig. 4a, the whole samples are identified by Type IV isotherms of the IUPAC classification. Reversible Type H2 (previously named Type E) hysteresis loops are also identified [94]. Such features attribute to the mesopores bearing capillary condensation [94]. The narrow pore size distribution of each sample is also confirmed by the results of Fig. 4b. Accordingly, each catalyst offers pores with overall identical sizes. The calculated pore sizes, surface areas, and pore volumes of the samples are summarized in Table 2. The average pore sizes of DC 130 CoMo, HDS 16A CoMo, TL 424 NiMo, and HDS 9A NiMo samples are 74 Å, 79 Å, 79 Å, and 105 Å, respectively. Moreover, the calculated BET surface areas of DC 130 CoMo, HDS 16A CoMo, TL 424 NiMo, and HDS 9A NiMo samples are 224.4 m^2/g, 137.1 m^2/g, 145.0 m^2/g, and 156.7 m^2/g, respectively.

3.2 Catalytic HDO of Cyclohexanone

The CoMo and NiMo catalysts are comparatively evaluated for the vapor-phase hydrodeoxygenation of cyclohexanone at 400 °C and 15 bar reaction temperature and pressure and WHSVs of 0.262–5.389 $g_{cyclohexanone}/g_{cat}$ h. The results of cyclohexanone conversion, product distribution, DDO%, and C/O RE are compared in this section. The complete experimental data of the conversion, selectivity, yield, C/O RE, and DDO% are reported in Tables S3 and S4 of the Supplemental Information. The typical carbon balance for the HDS 16A CoMo and HDS 9A NiMo samples are presented in the Table S2 of Supporting Information. A major source of the reported carbon balance deviations could be the carbon deposition on the catalyst surface.

The major common products of cyclohexanone HDO in the presence of hydrotreating catalysts were cyclohexane, cyclohexene, cyclohexanol, benzene, and phenol. Methylcyclopentane was also observed in some cases. Cyclohexylcyclohexanone and cyclohexylphenol were produced in the

Table 2 Catalysts surface area, pore volume, and pore size

Catalyst	Surface area (m^2/g)				Volume (cm^3/g)		Pore diameter (Å)
	BET	Langmuir	t-Plot (pore)	t-Plot (external)	t-Plot (micropore)	BJH	
DC 130 CoMo	224.4	307.6	41.3	183.1	0.0169	0.4616	74
HDS 16A CoMo	137.1	187.9	24.9	112.2	0.0105	0.3682	79
TL 424 NiMo	145.0	200.1	17.3	127.7	0.0066	0.3912	79
HDS 9A NiMo	156.7	215.3	28.6	128.0	0.0119	0.4622	105

case of the HDS 16A CoMo catalyst. Bicyclohexyl and cyclohexylbenzene were obtained by utilizing both NiMo catalysts.

Producing high-octane fuels would be a consequent utilization of cyclohexane, cyclohexene, benzene, and methylcyclopentane processing. Cyclohexane and cyclohexene are also commonly utilized to manufacture chemicals such as adipic acid, caprolactam, hexamethylenediamine, and the intermediates in the production of nylon. They may be employed as the dilutants of the polymeric reactions [95–102]. Benzene is widely utilized in manufacturing chemical s such as ethylbenzene, cumene, nitrobenzene, maleic anhydride, halogenated benzenes, and linear alkylbenzenes [103]. Cyclohexanol can be employed in the production of adipic acid and plasticizers, as a solvent, in the laundry industry, and the preparation of paint or varnish removers, insecticide, fragrance, and polish [104]. The production of chemicals such as bisphenol-A, polycarbonates, and epoxide resins, as well as molecular biology extractions, are of the major applications of phenol [105]. Multicyclic compounds such as cyclohexylbenzene, bicyclohexyl, cyclohexylcyclohexanone, and cyclohexylphenol are useful in further jet-fuel processing and nylons manufacturing [26, 106]. Based on the observed products, a lumped general reaction network is sketched in Fig. 5. The formation of each compound will be addressed in the following sections.

Figure 6 demonstrates the results of cyclohexanone conversion as a function of reaction WHSV and catalyst type. In the whole case, increasing WHSV resulted in steadily decreasing the conversion. This decrease in the conversion could be explained by the increase in reactant content for a fixed amount of catalyst. As WHSV is defined as the ratio of

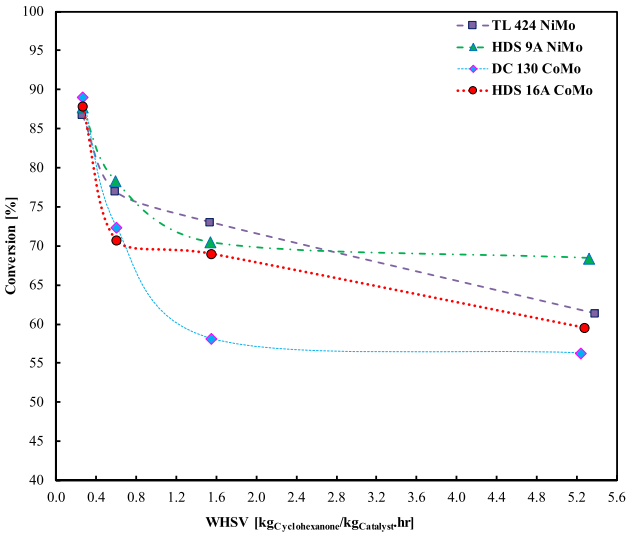

Fig. 6 Effect of catalyst type and WHSV on the conversion of cyclohexanone

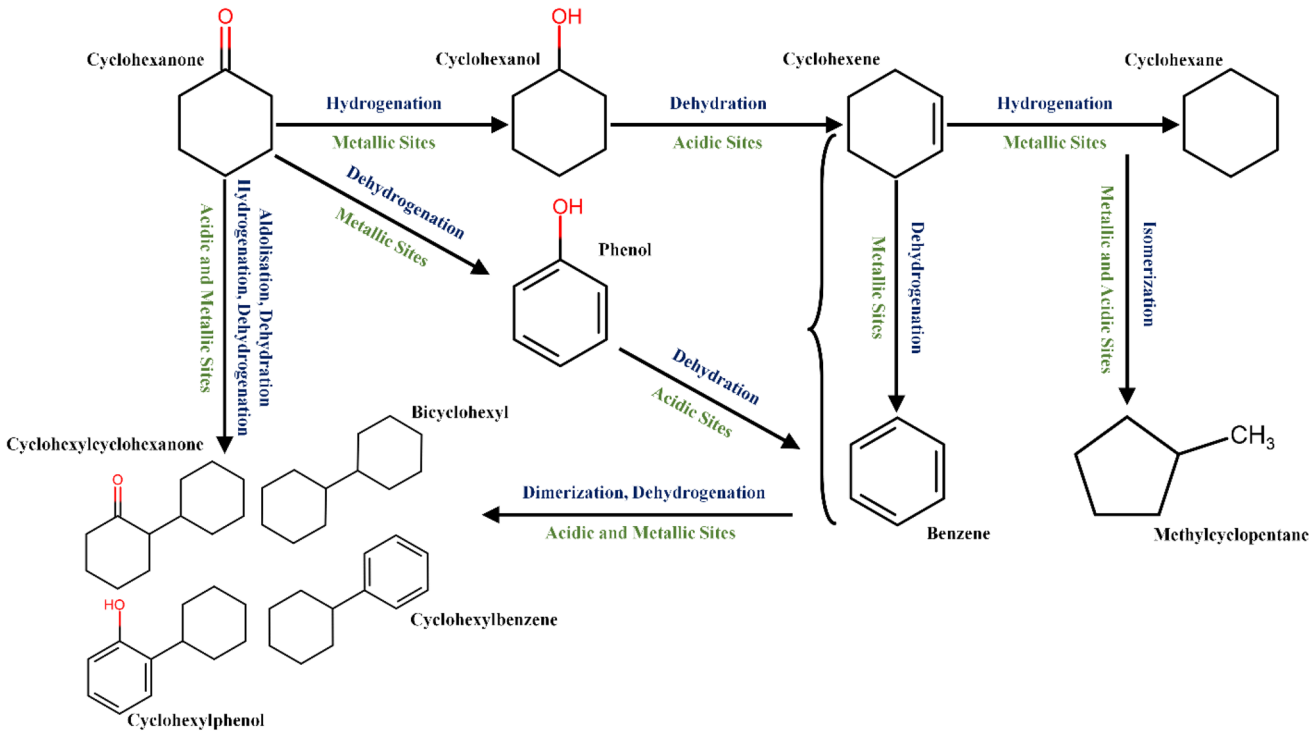

Fig. 5 The general lumped reaction system of the hydrodeoxygenation of cyclohexanone over CoMo and NiMo hydrotreating catalysts

cyclohexanone flowrate to the mass of catalyst, its increase resulted in the larger quantities of cyclohexanone in the vicinity of catalyst. Hence, the converted cyclohexanone decreased. In the high-conversion region, i.e. low WHSV ($\approx 0.26\ g_{cyclohexanone}/g_{cat}\ h$), the whole catalyst led to almost the same conversion. Accordingly, the conversion over DC 130 CoMo, HDS 16A CoMo, HDS 9A NiMo, and TL 424 NiMo catalysts are 89.04%, 87.87%, 87.77%, and 86.73%, respectively. As the reaction temperature and pressure are constant, conversion tends to the highest possible level at this condition, i.e. chemical equilibrium by increasing WHSV. This might imply that the Gibbs free energy is at the minimum level at this condition, where the multicomponent system reaches chemical equilibrium. Further increase of WHSV demonstrates the superiority of NiMo catalyst over CoMo ones in converting cyclohexanone. Sharp decays in the conversion followed gradual changes are observed in the whole cases. The most conversion decay with increasing WHSV is observed in the case of the DC 130 CoMo catalyst. As WHSV increased approximately 20 times larger, 32.75%, 28.32%, 19.35%, and 25.44% reductions in conversion were observed over DC 130 CoMo, HDS 16A CoMo, HDS 9A NiMo, and TL 424 NiMo catalysts, respectively. From a general point of view, catalyst composition, the ratio of the promoter (either nickel or cobalt) to the major catalytic species (molybdenum), acidity type and strength, and the textural properties including active surface area and pore volume affect the conversion differences.

Both catalyst type and reaction WHSV strongly influence the rates of the involved reactions. Hence, by changing the catalyst type and reaction WHSV, the effective reaction rates in the complex reaction system change significantly with different orders of magnitude. This would result in the qualitative and quantitative alteration of product distribution. The effect of WHSV on the distribution of the major products in the presence of HDS 16A CoMo, DC 130 CoMo, HDS 9A NiMo, and TL 424 NiMo catalysts are demonstrated in Figs. 7, 8, 9, 10. The results are compared in terms of selectivity and yield.

The results of product selectivity and yield over the HDS 16A CoMo catalyst are demonstrated in Fig. 7. The major products obtained by employing this catalyst include cyclohexane, cyclohexene, phenol, cyclohexanol, and cyclohexylphenol. However, small quantities of cyclohexylcyclohexanone were observed in some cases. Methylcyclopentane and benzene were not observed in the experimented conditions.

Based on the observed products, the reaction pathway for the HDO conversion of cyclohexanone can be classified into two routes, the first of which includes the formation of C_6 cyclic compounds. The latter includes the formation of C_{12} bicyclic compounds. Both routes may result in the formation of deoxygenated products. The first route in detail

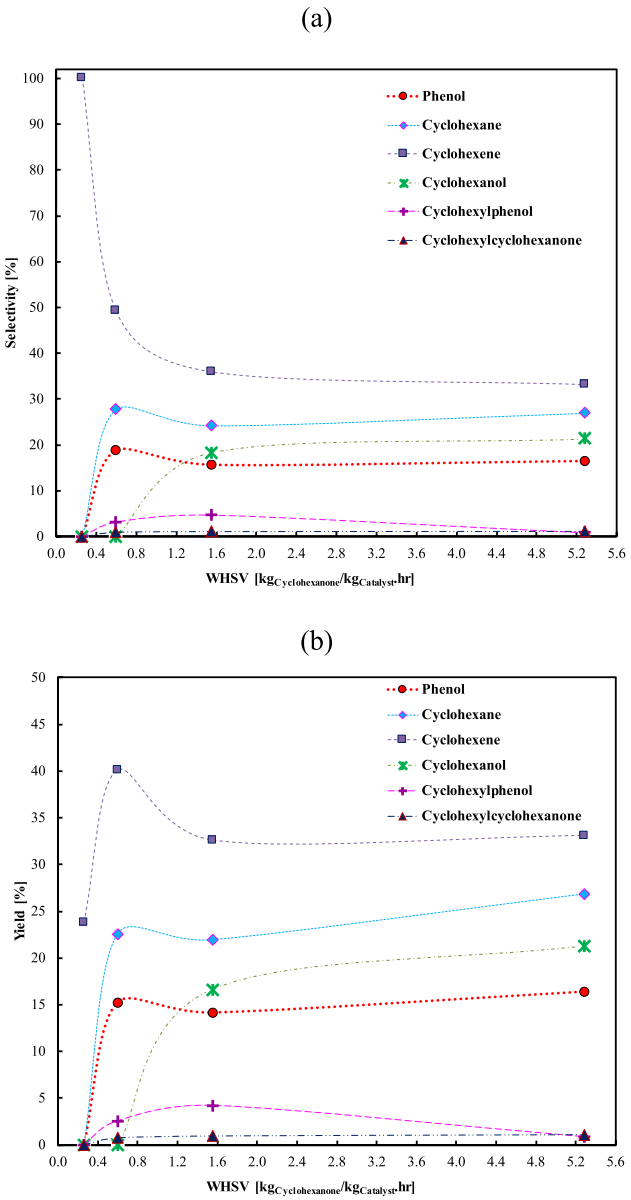

Fig. 7 Product selectivity (**a**) and yield (**b**) in the conversion of cyclohexanone over HDS 16A CoMo catalyst

includes the hydrogenation of cyclohexanone to cyclohexanol on the metallic sites of the catalyst. Then, the dehydration (or dehydroxylation) of cyclohexanol on the acidic sites of the catalyst leads to the formation of cyclohexene. Further hydrogenation of cyclohexene on the metallic sites generates cyclohexane. The direct dehydrogenation of cyclohexanone on the metallic sites produces phenol. The characterization results addressed in the previous sections proved the presence of both metallic and acid sites in the catalyst structure. Alvarez et al. [44] discussed the transformation of cyclohexanone on metallic and acidic sites. The second reaction route that results in the formation of

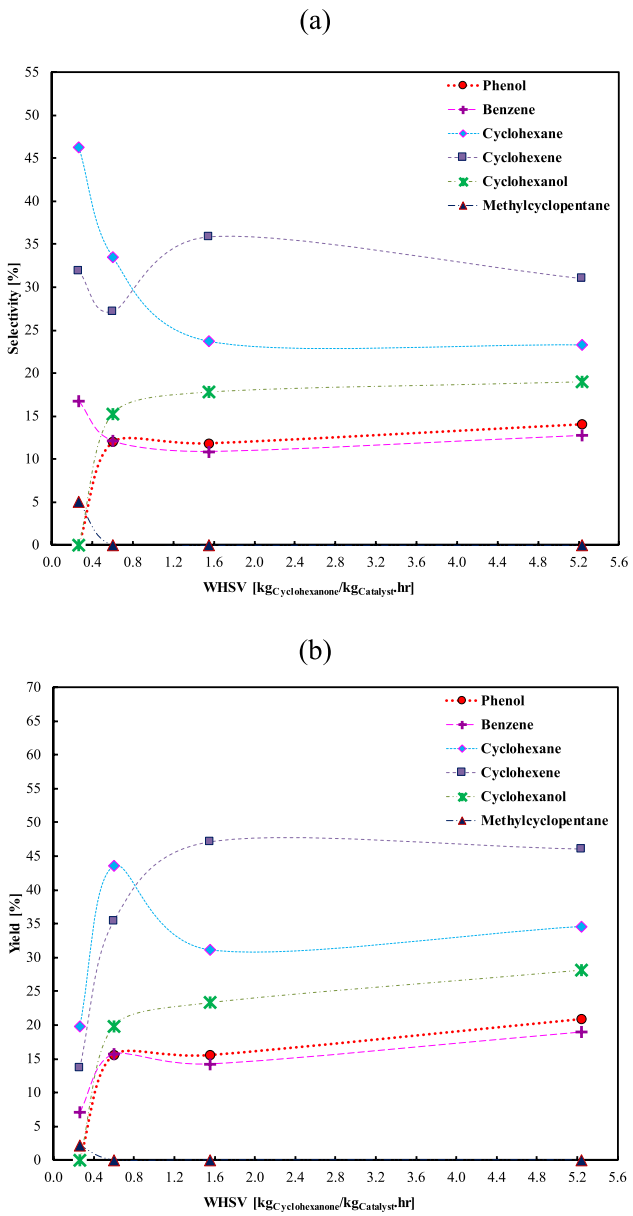

Fig. 8 Product selectivity (**a**) and yield (**b**) in the conversion of cyclohexanone over DC 130 CoMo catalyst

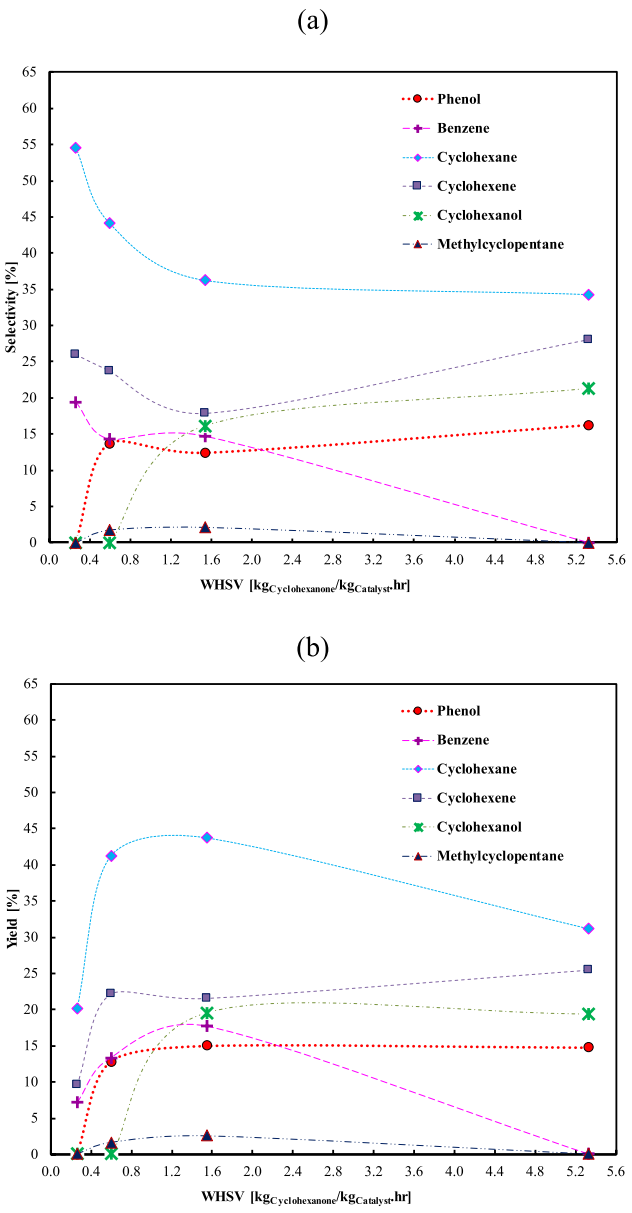

Fig. 9 Product selectivity (**a**) and yield (**b**) in the conversion of cyclohexanone over HDS 9A NiMo catalyst

C_{12} bicyclic compounds includes a set of consecutive reactions. This route includes a primary aldol condensation of cyclohexanone on the acidic sites of the catalyst. Then, the dehydration of the intermediate alcohol on the acidic sites produces cyclohexenylcyclohexanone. The hydrogenation of cyclohexenylcyclohexanone on the metallic sites produces cyclohexylcyclohexanone. Successive dehydrogenation of cyclohexylcyclohexanone on the metallic sites generates cyclohexylphenol [44]. It is worth noting that the dimerization of the as-formed C_6 monocyclic compounds in the first reaction path and their further transformation may also produce the C_{12} bicyclic compounds. Based on the observations of Alvarez et al. [44], the high-temperature reaction on the strong acidic sites often enhances the generation of bicyclic compounds. The presence of strong acidic sites in the HDS 16A CoMo catalyst was proved in the previous sections (Fig. 3).

As per Fig. 7a, at the lowest WHSV (0.262 $g_{cyclohexanone}/g_{cat}$ h), i.e. the highest conversion, the only observed product was cyclohexene, which means that the reactions leading to the formation of cyclohexene (the hydrogenation of to cyclohexanol, then its dehydration to cyclohexene) are dominant in the high-conversion condition. An increase of the reaction WHSV (0.599 $g_{cyclohexanone}/g_{cat}$ h) leads to a sharp

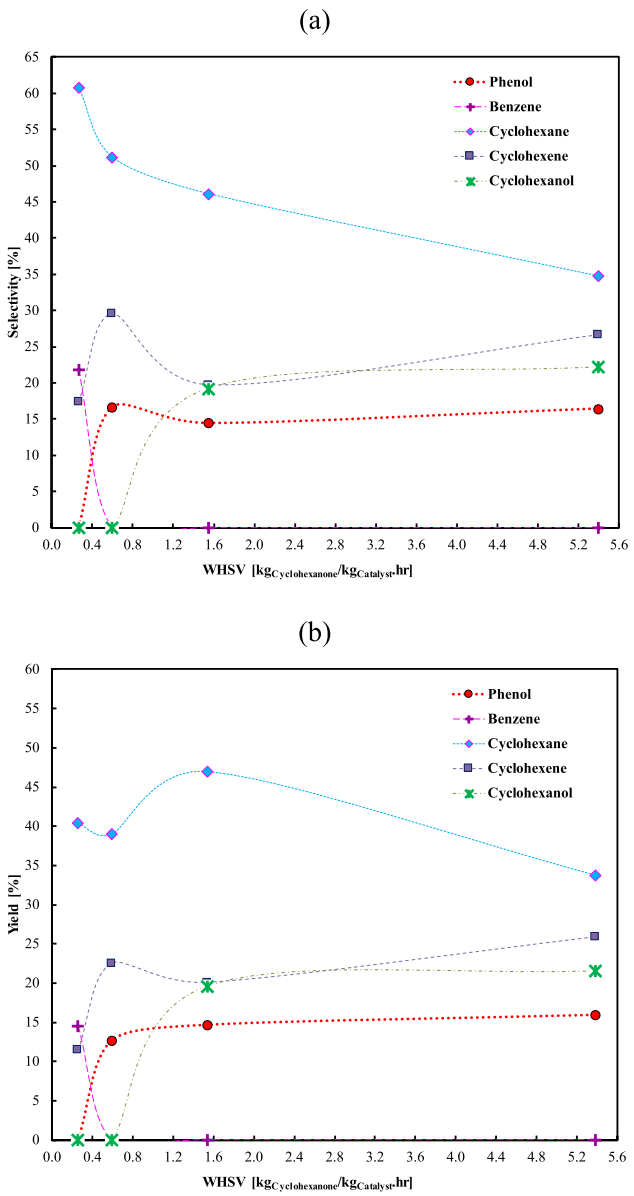

Fig. 10 Product selectivity (**a**) and yield (**b**) in the conversion of cyclohexanone over TL 424 NiMo catalyst

reduction of cyclohexene selectivity and an increase in the selectivities of cyclohexane and phenol. On the one hand, by increasing WHSV, the rates of direct dehydrogenation of cyclohexanone to phenol, as well as the conversion of cyclohexene to cyclohexane, is enhanced. Further increase of the reaction WHSV 1.551 $g_{cyclohexanone}/g_{cat}$ h enhances the formation of cyclohexanol and thus dampens the formation of cyclohexane and phenol. A further increase of the reaction WHSV up to 5.282 $g_{cyclohexanone}/g_{cat}$ h does not change the relative reaction rates and product selectivities, notably. At this reaction condition, the selectivities of cyclohexene, cyclohexane, cyclohexanol, and phenol are 33.23%, 26.97%, 21.35%, and 16.47%, respectively. It is also worth mentioning that 100.00–60.20% of the produced compounds at WHSV = 0.262–5.282 $g_{cyclohexanone}/g_{cat}$ h is made up of cyclohexane and cyclohexene.

Figure 7b demonstrates the results of product yields in the conversion of cyclohexanone over the HDS 16A CoMo. In the experimented conditions, the production yields of cyclohexane and cyclohexene are 0.00–26.89% and 23.80–40.15%, respectively. Noteworthily, 23.80–62.74 mol of cyclohexane and cyclohexene would be produced in tandem per 100 mol of cyclohexanone conversion at 400 °C, 15 bar, and the experimented WHSV range. At the same reaction condition, the yields of phenol and cyclohexanol are 0.00–16.42% and 0.00–21.35%, respectively. It is worth mentioning that benzene was not observed over the HDS 16A CoMo catalyst. On the other hand, 15 bar reaction pressure, i.e. the higher hydrogen partial pressure in the reaction media inhibited the further dehydrogenation of cyclohexene to benzene.

The results of product selectivity and yield over the DC 130 CoMo catalyst are depicted in Fig. 8. The major products obtained when cyclohexanone is converted by this catalyst involve cyclohexane, cyclohexene, benzene, cyclohexanol, and phenol. However, a small quantity of methylcyclopentane was produced in the lowest WHSV. Bicyclic compounds were not produced in the experimented conditions. The reaction route leading to the formation of cyclohexene, cyclohexane, cyclohexanol, and phenol was well addressed in the aforementioned discussions. Benzene is produced through the further dehydrogenation of cyclohexene on the metallic sites of the catalyst. The results reveal that benzene might be produced by the dehydroxylation of as-produced phenol on the acidic sites. Furthermore, as a result of the isomerization of cyclohexene and cyclohexane [44], a small quantity of methylcyclopentane was also observed. Both acidic and metallic sites of the catalyst are responsible for this transformation.

As depicted in Fig. 8a, at the lowest WHSV (0.263 $g_{cyclohexanone}/g_{cat}$ h) and thus the highest conversion, cyclohexane is the major obtained product. At this reaction condition, cyclohexene, benzene, and methylcyclopentane were also generated. No phenol and cyclohexanol were generated in this condition. The whole formed cyclohexanol is converted at this reaction condition. It is inferred that the successive reactions leading to the formation of cyclohexene intermediate are dominant in the high-conversion condition. Cyclohexene is then converted to benzene, cyclohexane, and methylcyclopentane. The selectivities of cyclohexane, cyclohexene, benzene, and methylcyclopentane are 46.28%, 31.91%, 16.76%, and 5.06%, respectively.

If we compare the productions of cyclohexane, cyclohexene, and benzene over the DC 130 CoMo sample with those of the HDS 16A sample, it is revealed that the hydrogenation of cyclohexene to cyclohexane and their dehydrogenation to

benzene are enhanced over DC 130 CoMo. As discussed earlier, these reactions occur on the metallic sites of the catalyst and the results of elemental analysis (Table 1) depict that the DC 130 CoMo sample is made up of larger quantities of metallic catalytic species. DC 130 CoMo sample is made up of 18.37% of Co and Mo, while the HDS 16A CoMo sample includes 14.82% of Co and Mo. Hence, the larger quantity of the catalytic metallics in the catalyst structure enhanced the hydrogenation of cyclohexene to cyclohexane and their dehydrogenation to benzene. Moreover, the NH_3-TPD results of HDS 16A and DC 130 CoMo samples (Fig. 3 and Table 1) demonstrate that there are differences in the strong acidity region as well as the total quantity of catalyst acidity. Such differences affected the formation of bicyclic compounds in the HDO of cyclohexanone over these two samples. As discussed earlier, strong acidic sited catalyze the formation of bicyclics. Hence, employing the DC 130 CoMo sample with less-strong acidity and less acidic sites does not produce bicyclics.

An increase of WHSV (0.600 $g_{cyclohexanone}/g_{cat}$ h) results in the reduction of cyclohexane, cyclohexene, and benzene selectivities as well as the formation of phenol and cyclohexanol. On the other hand, a portion of the cyclohexanol intermediate was converted to cyclohexene and cyclohexane. The trends of phenol and benzene also reveal that benzene might be generated through the dehydroxylation of the as-produced phenol. Hence, by increasing WHSV (reduction of conversion), the transformation of phenol to benzene is inhibited. The formation of methylcyclopentane is also dampened in this reaction condition. A further increase in the reaction WHSV up to 1.544 $g_{cyclohexanone}/g_{cat}$ h does not change the selectivities of benzene, phenol, and cyclohexanol. However, the formation of cyclohexene is enhanced, while the cyclohexene selectivity decreases in this reaction. At this reaction condition, the hydrogenation of cyclohexene to cyclohexane is inhibited, and thus the selectivity of cyclohexene increases. By a further increase of the reaction WHSV up to 5.240 $g_{cyclohexanone}/g_{cat}$ h, the relative rates of the whole reactions are almost constant. At this reaction condition, the selectivities of cyclohexene, cyclohexane, cyclohexanol, phenol, and benzene are 31.01%, 23.27%, 18.95%, 14.04%, and 12.37%, respectively. It would be interesting to note that 78.18–54.28% of the produced compounds at WHSV = 0.263–5.240 $g_{cyclohexanone}/g_{cat}$ h is made up of cyclohexane and cyclohexene.

As per Fig. 8b, in the experimented conditions, the production yields of cyclohexane and cyclohexene are 19.73–43.51% and 13.60–47.12%, respectively. Moreover, 33.33–80.62 mol of cyclohexane and cyclohexene can be produced in tandem when 100 mol of cyclohexanone is converted at 400 °C, 15 bar, and the examined WHSV range. At the same reaction condition, the production yields of benzene, cyclohexanol, and phenol 7.14–18.91%, 0.00–28.15%, and 0.00–20.85%, respectively. This confirms that the dehydration of cyclohexanol is a very fast step at higher conversions. It is worth noting that increasing WHSV results in the lower conversion of cyclohexanone as well as the formation of products that are suitable for further fuel processing.

The results of product selectivity and yield over the HDS 9A NiMo catalyst are depicted in Fig. 9. Cyclohexane, cyclohexene, benzene, phenol, and cyclohexanol are the major products obtained by employing this catalyst. However, small quantities of methylcyclopentane, bicyclohexyl, and cyclohexylbenzene were obtained in some tested conditions. The reaction path leading to the formation of cyclohexene, cyclohexane, cyclohexanol, benzene, phenol, and methylcyclopentane were discussed earlier. The observed C_{12} bicyclic hydrocarbons, i.e. bicyclohexyl and cyclohexylbenzene would be produced through the deoxygenation of the as-produced C_{12} bicyclic oxygenates or the initial dimerization of the as-produced C_6 hydrocarbons and their further transformations [44].

As demonstrated in Fig. 9a, at the lowest WHSV (0.264 $g_{cyclohexanone}/g_{cat}$ h), i.e. the highest conversion, the major product is cyclohexane. At the same reaction condition, cyclohexene and benzene were also produced. Phenol, cyclohexanol, and methylcyclopentane were not formed in this condition. The whole formed cyclohexanol and phenol might be converted to cyclohexene and benzene, respectively. Hence, the consecutive reactions to produce cyclohexene, cyclohexane, and benzene are dominant in the high-conversion region. The selectivities of cyclohexane, cyclohexene, and benzene are 54.56%, 26.03%, and 19.42%, respectively. An increase of the reaction WHSV (0.594 $g_{cyclohexanone}/g_{cat}$ h) changes the reaction path toward the formation of phenol and a small quantity of methylcyclopentane. Simultaneous formation of phenol and the reduction of benzene, cyclohexane, and cyclohexene reveal that phenol is produced from the direct dehydrogenation of cyclohexanone. A larger portion of cyclohexanone, on the one hand, takes part in the direct dehydrogenation into phenol rather than the transformation into cyclohexene, cyclohexane, and benzene. The formation of methylcyclopentane is also responsible for a portion of reduced selectivities of cyclohexane, cyclohexene, and benzene. Cyclohexanol appears with 16.17% selectivity when WHSV increases to 1.542 $g_{cyclohexanone}/g_{cat}$ h. The formation of cyclohexanol, while the benzene and phenol selectivities are almost constant, infers that the rate of cyclohexanol dehydration to cyclohexene was dampened by increasing WHSV. Increasing WHSV up to 5.324 $g_{cyclohexanone}/g_{cat}$ h led to the total conversion of the as-produced benzene to phenol and cyclohexene. At this reaction condition, no benzene was observed. Unlike the CoMo catalyst, increasing WHSV beyond 5.000 $g_{cyclohexanone}/g_{cat}$ h does not lead to the balanced relative reaction rates. At the highest reaction WHSV (5.324 $g_{cyclohexanone}/g_{cat}$ h), i.e. the lowest

cyclohexanone conversion, the selectivities of cyclohexane, cyclohexene, cyclohexanol, and phenol are 34.32%, 28.09%, 21.23%, and 16.27%, respectively. Moreover, 80.58–54.16% of the produced compounds at the experimented condition involve cyclohexane and cyclohexene.

The results of product yields in the conversion of cyclohexanone over the HDS 9A NiMo catalyst are addressed in Fig. 9b. In the experimented conditions, the production yields of cyclohexane, cyclohexene, benzene, phenol, and cyclohexanol are 43.74–20.05%, 9.57–25.49%, 0.00–17.73%, 0.00–15.00%, and 0.00–19.50%, respectively. The yields of methylcyclopentane and total bicyclic hydrocarbons (bicyclohexyl and cyclohexylbenzene) are up to 2.54% and 2.08%, respectively. Noteworthily, 29.62–65.31 mol of cyclohexane and cyclohexene can be produced in tandem per 100 mol of cyclohexanone conversion at 400 °C, 15 bar, and the experimented WHSV range.

Figure 10 depicts the product distribution of cyclohexanone conversion over the TL 424 NiMo catalyst. The major products of cyclohexanone HDO over this catalyst include cyclohexane, cyclohexene, phenol, and cyclohexanol. Benzene, bicyclohexyl, and cyclohexylbenzene were also generated in some tested conditions. The reactions that are responsible for the formation of these products have been addressed previously.

As per Fig. 10a, at the lowest WHSV (0.262 $g_{cyclohexanone}/g_{cat}$ h) and thus the highest conversion, a considerable quantity of cyclohexane (60.79%) is produced. Benzene and cyclohexene are produced with 21.84% and 17.31% shares, respectively. Phenol, cyclohexanol, and bicyclics were not formed in this reaction condition. At the higher WHSV (0.597 $g_{cyclohexanone}/g_{cat}$ h), the selectivity of cyclohexane decrease, while a larger quantity of cyclohexene is formed. Moreover, no benzene is formed in this condition. Hence, the conversion of cyclohexene to cyclohexane and benzene is dampened in this condition. Moreover, the dehydroxylation of phenol to benzene is also controlled. No cyclohexanol is formed in this condition too. Further increase of WHSV to 1.542 $g_{cyclohexanone}/g_{cat}$ h resulted in the generation of cyclohexanol as well as the reduced cyclohexane and cyclohexene quantities, while the selectivity of phenol is almost constant. Such a change in reaction WHSV controls the further transformation of cyclohexanol intermediate to the subsequent products, i.e. cyclohexene and cyclohexane. In the higher reaction WHSV (5.389 $g_{cyclohexanone}/g_{cat}$ h), the relative rates of phenol and cyclohexanol production become constant, while cyclohexene conversion to cyclohexane is further controlled. Unlike the CoMo samples, increasing WHSV beyond 5.000 $g_{cyclohexanone}/g_{cat}$ h does not balance the relative reaction rates. At this reaction condition, 34.75%, 26.64%, 22.19%, and 16.42% of the final product is made up of cyclohexane, cyclohexene, cyclohexanol, and phenol, respectively. Furthermore, 61.39–80.69% of the products include cyclohexane and cyclohexene at the experimented range.

Figure 10b addresses the results of product yields in the HDO of cyclohexanone over the TL 424 NiMo catalyst. In the examined conditions, the production yields of cyclohexane, cyclohexene, benzene, phenol, and cyclohexanol are 33.78–47.00%, 11.55–25.89%, 0.00–14.52%, 0.00–15.96%, and 0.00–21.56%, respectively. The yield of total bicyclic hydrocarbons (bicyclohexyl and cyclohexylbenzene) is up to 2.01%. It is interesting to note that per 100 mol of the converted cyclohexanone, 51.96–67.11 mol of cyclohexane and cyclohexene would be produced in tandem at 400 °C, 15 bar, and the examined WHSV range.

The impact of the catalysts on the production of cyclohexane and cyclohexene is addressed in Fig. 11. As discussed earlier, the dehydration of cyclohexanol on the acidic sites of the catalyst produces cyclohexene. Figure 11 reveals that the performance of the HDS 16A CoMo catalyst is different at the highest conversion (i.e. the lowest WHSV). At this condition, cyclohexene is produced and its further dehydrogenation does not proceed. The dehydration of cyclohexanol to cyclohexene on the acidic sites, on the one hand, overcomes the further dehydrogenation on the metallic sites. As per Table 1, the HDS 16A CoMo possesses the smallest quantity of metallic content (14.82 wt.%). Hence, the dehydration reaction over this catalyst is dominant. The selectivities of cyclohexene over this catalyst are then larger in almost all the examined WHSV range. When compared to the HDS 16A CoMo sample, the DC 130 CoMo catalyst possesses a higher metal content and a lower acidity. The ratio of the promoter (i.e. Co) to the main metal (Mo) is also larger in the DC 130 CoMo sample. These resulted in the production of larger quantities of cyclohexane over DC 130 CoMo catalyst. Figure 11 also reveals that the synergistic effect of Ni and Mo resulted in the production of larger quantities of cyclohexane in the whole examined WHSV range.

Although the whole obtained products as a result of cyclohexanone conversion are value-added, the main goal of this process is the enhancement of carbon to oxygen ratio. This would prepare streams that are suitable for further fuel processing. Hence, the results of deoxygenation and total hydrocarbon production are of notable importance for further decision making. In this regard, the results of deoxygenation criteria and total hydrocarbon production are demonstrated in Figs. 12 and 13, respectively.

Figure 12 depicts the impacts of catalyst type and WHSV on DDO% and C/O RE. All the examined catalysts offer the highest deoxygenation in the highest conversion, i.e. the lowest WHSV. Increasing WHSV leads to lower deoxygenation rates. By increasing the WHSV, the rates of the reaction that are responsible for deoxygenation are on the other hand controlled. The highest DDO% (81.29%) and C/O RE (5.35) were obtained by TL 424 NiMo catalyst. However, the C/O

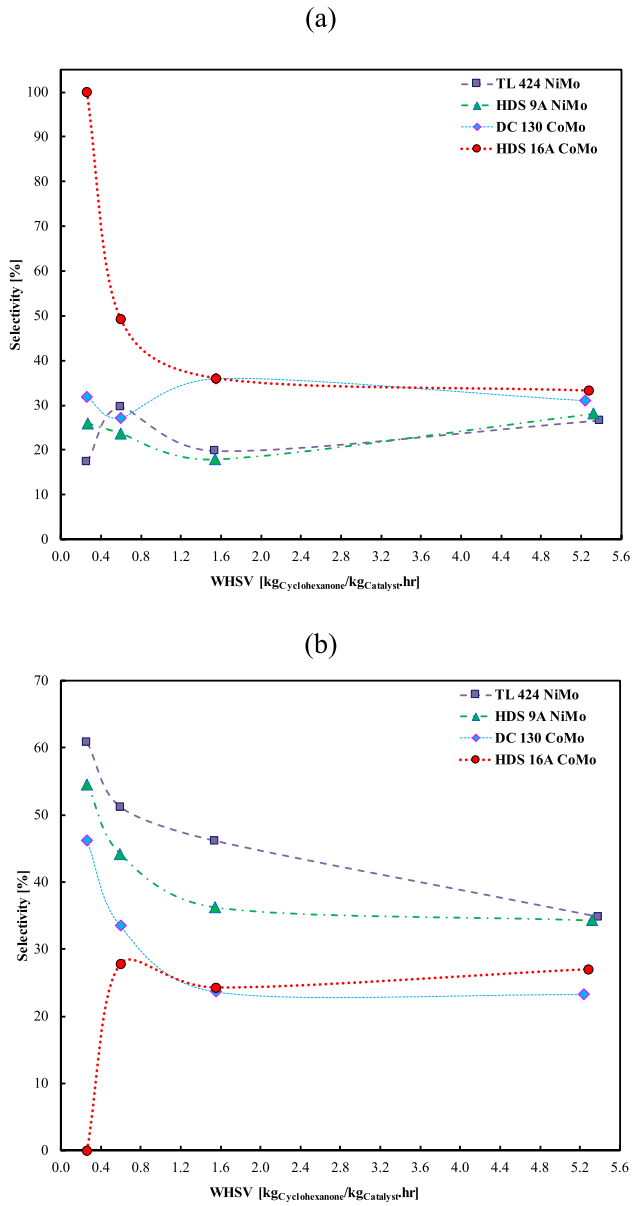

Fig. 11 Effect of catalyst type and WHSV on the selectivities of cyclohexene (**a**) and cyclohexane (**b**)

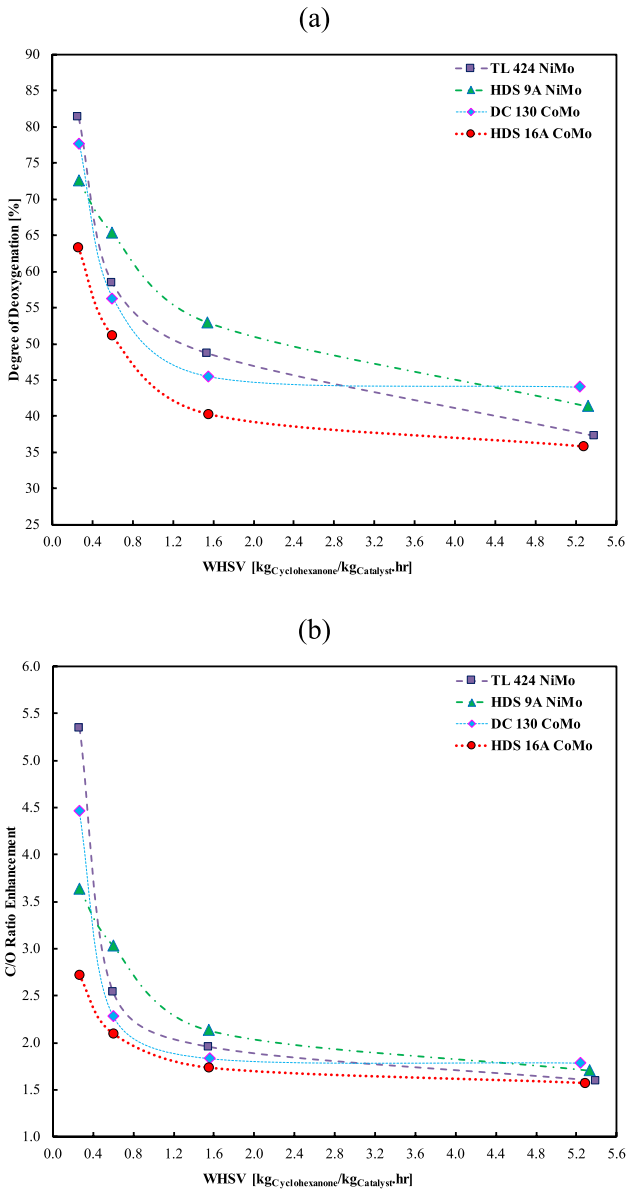

Fig. 12 Effect of catalyst type and WHSV on the degree of deoxygenation (**a**) and C/O ratio enhancement (**b**)

RE of greater than 1 in the whole cases reveals the success of the process in the upgrading of cyclohexanone to the fuel-grade products.

The impacts of catalyst type and WHSV on the total hydrocarbon selectivity and yield are addressed in Fig. 13. Clearly, in the high-conversion region, the whole products are hydrocarbon, i.e. the total hydrocarbon selectivity is 100%. However, the largest hydrocarbon productivity was obtained in different conditions. Increasing the reaction WHSV results in the dominance of the non-deoxygenating reactions. The minimum total hydrocarbon yields for all the catalysts were obtained in the high-conversion region, i.e. low WHSVs. DC 130 CoMo catalyst produces the largest quantities of total hydrocarbons in the larger WHSVs. The largest hydrocarbon production capacity was obtained by employing DC 130 CoMo catalyst. 99.53% total hydrocarbon yield was achieved by upgrading cyclohexanone over DC 130 CoMo catalyst at 400 °C, 15 bar, and 5.240 $g_{cyclohexanone}/g_{cat}$ h. While the best deoxygenation performance was obtained by employing TL 424 NiMo at 0.262 $g_{cyclohexanone}/g_{cat}$ h.

As discussed earlier, the main objective of cyclohexanone HDO is the production of liquid fuel-grade products. Hence, it would be beneficial to assess and compare the heating values (HHV and LHV) of the products. To do

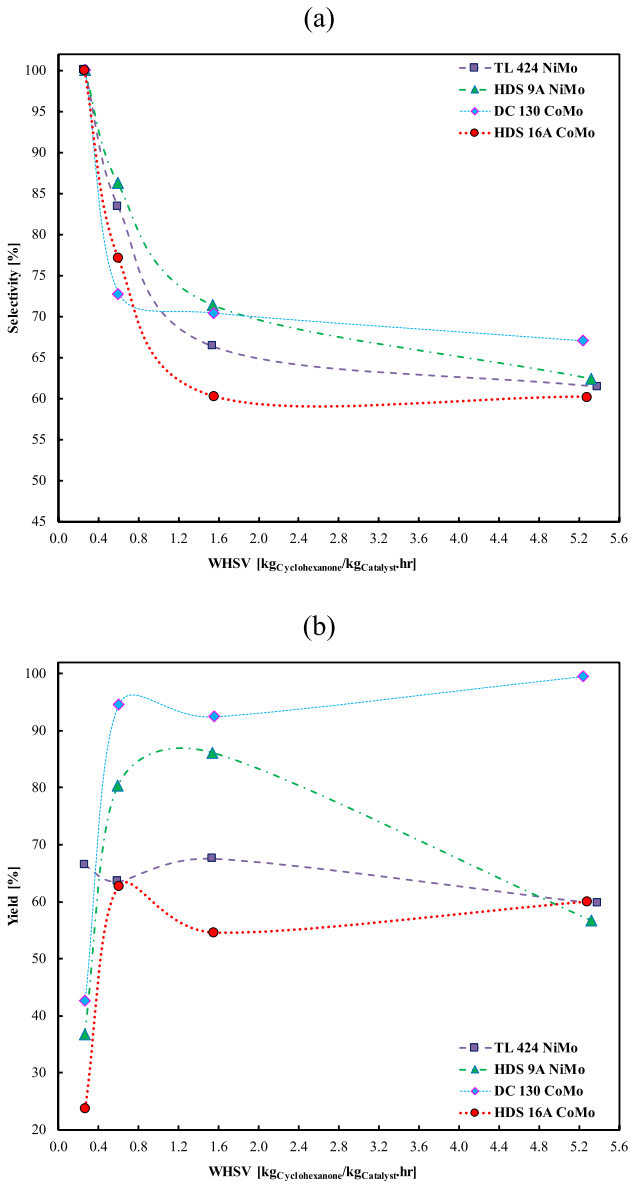

Fig. 13 Effect of catalyst type and WHSV on the total hydrocarbon selectivity (**a**) and yield (**b**)

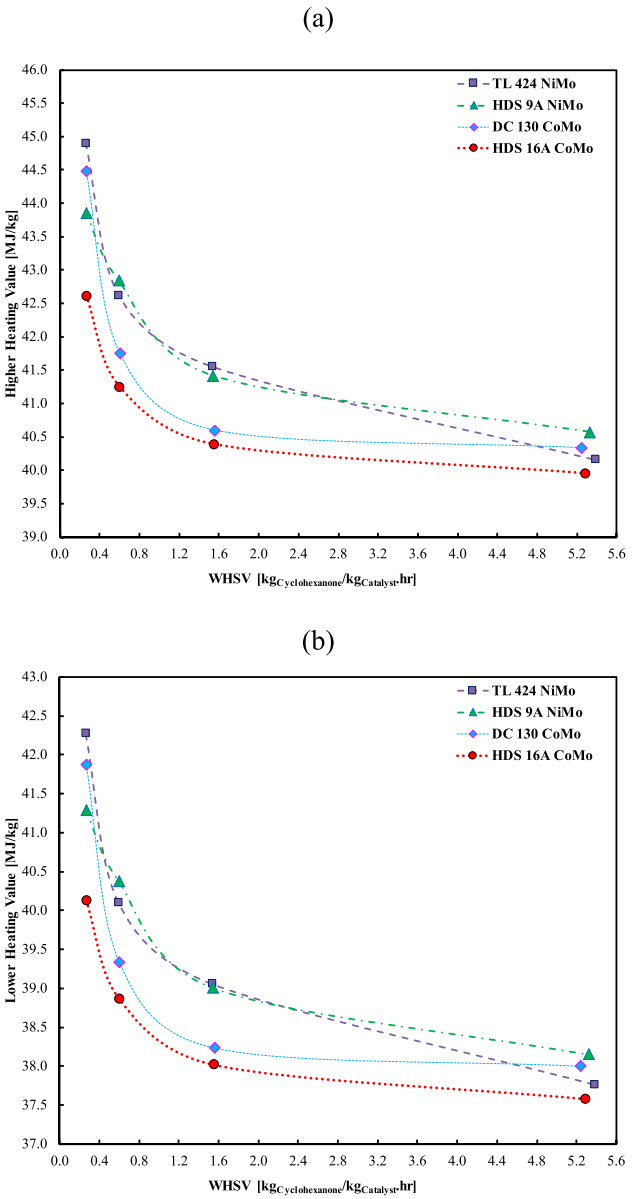

Fig. 14 Effect of catalyst type and WHSV on the higher heating value (**a**) and lower heating value (**b**) of the product blends

so, Fig. 14 is depicted. The results reveal that the HHVs of the obtained blends are in the range of 39.96–42.61 MJ/kg, 40.34–44.48 MJ/kg, 40.57–43.86 MJ/kg, and 40.16–44.90 MJ/kg when cyclohexanone is converted over HDS 16A CoMo, DC 130 CoMo, HDS 9A NiMo, and TL 424 NiMo, respectively. LHVs are in the range of 37.58–40.13 MJ/kg, 38.00–41.87 MJ/kg, 38.15–41.29 MJ/kg, and 37.75–42.27 MJ/kg, respectively. Cyclohexanone conversion, deoxygenation efficiency, and product distribution affect the heating values of the product blends. Accordingly, when compared to cyclohexanone (HHV = 36.62 MJ/kg), HHVs of the product blends would be enhanced by 16.5%, 21.6%, 19.9%, and 22.7% when cyclohexanone is converted at the lowest WHSV (≈0.26 $g_{cyclohexanone}/g_{cat}$ h) over HDS 16A CoMo, DC 130 CoMo, HDS 9A NiMo, and TL 424 NiMo, respectively. The largest heat value (HHV = 44.90 MJ/kg, 22.7% enhancement) was obtained by the conversion of cyclohexanone over the TL 424 NiMo catalyst at 0.262 $g_{cyclohexanone}/g_{cat}$ h. The obtained HHVs are comparable with the energy contents of conventional fuels such as aviation gasoline (46.8 MJ/kg), automotive diesel (45.6 MJ/kg), and automotive gasoline (46.4 MJ/kg) as well as combustible alcohols such as methanol (19.7 MJ/kg) and ethanol (29.6 MJ/kg) [6]. Hence, the obtained product of cyclohexanone HDO over the assessed molybdenum-based catalysts can be then utilized as an energy resource.

4 Conclusions

Developing biomass-derived fuels is a promising means for eliminating the harmful effects of conventional fuels and further global warming. To do so, the conversion of lignin-derived intermediates such as cyclohexanone is a major trend. Prompted this need, the commercial CoMo and NiMo catalysts were characterized and compared for the hydrodeoxygenation of cyclohexanone. The cyclohexanone upgrading to fuel-grade hydrocarbons at 400 °C, 15 bar total pressure, and a range of WHSV were addressed and discussed. Moreover, the impacts of catalyst type and WHSV on the cyclohexanone conversion, product distribution, deoxygenation efficiency, and total hydrocarbon production capacity were investigated. The investigated catalysts propose a high activity, selectivity, and yield for the upgrading of cyclohexanone to fuel-grade streams. The major produced components included C_6 cyclic and aromatic hydrocarbons. Cyclohexane, cyclohexene, and benzene were the major produced hydrocarbons. However, considerable quantities of oxygenates such as phenol and cyclohexanol were obtained in some experiments. A simple and general lumped reaction network covering the current observations was then presented. According to the observations, by increasing WHSV, cyclohexanone conversion decreased. The highest cyclohexanone conversions, i.e. greater than 86% were obtained at WHSV≈0.26 $g_{cyclohexanone}/g_{cat}$ h. The catalyst type and reaction WHSV had major impacts on product distribution, deoxygenation efficiency, and total hydrocarbon production capacity. The highest hydrocarbon yield (99.53%) was obtained at WHSV = 5.240 $g_{cyclohexanone}/g_{cat}$ h over a CoMo sample, while the highest DDO% (81.29%) and C/O ratio enhancement (5.35) were observed at WHSV = 0.262 $g_{cyclohexanone}/g_{cat}$ h over a NiMo sample. An assessment of heating values revealed that up to 22.7% enhancement in the HHV of the final product can be obtained. The larger HHV (44.90 MJ/kg) is comparable with the energy contents of conventional fuels. Therefore, the results of the present contribution proved the efficient performance of the CoMo and NiMo hydrotreating catalysts in the upgrading of cyclohexanone to fuel-grade streams.

Supplementary Information The online version contains supplementary material available at https://doi.org/10.1007/s10562-021-03575-y.

Acknowledgements The authors would like to thank Shiraz University for providing research facilities in the completion of the present study.

Compliance with Ethical Standards

Conflict of interest The authors whose names are listed in the manuscript certify that they declare no present and/or future conflict of interest.

References

1. Ellabban O, Abu-Rub H, Blaabjerg F (2014) Renewable energy resources: current status, future prospects and their enabling technology. Renew Sustain Energy Rev 39:748–764
2. Azadi P, Inderwildi OR, Farnood R, King DA (2013) Liquid fuels, hydrogen and chemicals from lignin: a critical review. Renew Sustain Energy Rev 21:506–523
3. Saidi M, Samimi F, Karimipourfard D, Nimmanwudipong T, Gates BC, Rahimpour MR (2014) Upgrading of lignin-derived bio-oils by catalytic hydrodeoxygenation. Energy Environ Sci 7(1):103–129
4. Espinoza-Acosta JL, Torres-Chávez PI, Olmedo-Martínez JL, Vega-Rios A, Flores-Gallardo S, Zaragoza-Contreras EA (2018) Lignin in storage and renewable energy applications: a review. J Energy Chem 27(5):1422–1438
5. Bridgwater AV (2012) Review of fast pyrolysis of biomass and product upgrading. Biomass Bioenergy 38:68–94
6. Bakhtyari A, Makarem MA, Rahimpour MR (2019) Hydrogen production through pyrolysis. In: Lipman TE, Weber AZ (eds) Fuel cells and hydrogen production: a the encyclopedia of sustainability science and technology, Second. Springer, New York, NY, pp 947–73
7. Bakhtyari A, Makarem MA, Rahimpour MR (2017) 4—Light olefins/bio-gasoline production from biomass. In: Dalena F, Basile A, Rossi C (eds) Bioenergy systems for the future. Woodhead Publishing, Kidlington, pp 87–148
8. Ma J, Shi S, Jia X, Xia F, Ma H, Gao J et al (2019) Advances in catalytic conversion of lignocellulose to chemicals and liquid fuels. J Energy Chem 36:74–86
9. Corma A, Iborra S, Velty A (2007) Chemical routes for the transformation of biomass into chemicals. Chem Rev 107(6):2411–2502
10. Kucherov FA, Romashov LV, Galkin KI, Ananikov VP (2018) Chemical transformations of biomass-derived C6-furanic platform chemicals for sustainable energy research, materials science, and synthetic building blocks. ACS Sustain Chem Eng 6(7):8064–8092
11. Iris K, Tsang DC (2017) Conversion of biomass to hydroxymethylfurfural: a review of catalytic systems and underlying mechanisms. Biores Technol 238:716–732
12. Hu X, Gholizadeh M (2019) Biomass pyrolysis: a review of the process development and challenges from initial researches up to the commercialisation stage. J Energy Chem 39:109–143
13. Chen H, Liu J, Chang X, Chen D, Xue Y, Liu P et al (2017) A review on the pretreatment of lignocellulose for high-value chemicals. Fuel Process Technol 160:196–206
14. Kumar B, Bhardwaj N, Agrawal K, Chaturvedi V, Verma P (2020) Current perspective on pretreatment technologies using lignocellulosic biomass: an emerging biorefinery concept. Fuel Process Technol 199:106244
15. Chen X, Che Q, Li S, Liu Z, Yang H, Chen Y et al (2019) Recent developments in lignocellulosic biomass catalytic fast pyrolysis: strategies for the optimization of bio-oil quality and yield. Fuel Process Technol 196:106180
16. Rahman MM, Liu R, Cai J (2018) Catalytic fast pyrolysis of biomass over zeolites for high quality bio-oil–a review. Fuel Process Technol 180:32–46
17. Zhou M, Sharma BK, Li J, Zhao J, Xu J, Jiang J (2019) Catalytic valorization of lignin to liquid fuels over solid acid catalyst assisted by microwave heating. Fuel 239:239–244
18. Luterbacher J, Alonso DM, Dumesic J (2014) Targeted chemical upgrading of lignocellulosic biomass to platform molecules. Green Chem 16(12):4816–4838

19. Sun Z, Bottari G, Afanasenko A, Stuart MC, Deuss PJ, Fridrich B et al (2018) Complete lignocellulose conversion with integrated catalyst recycling yielding valuable aromatics and fuels. Nat Catal 1(1):82–92
20. Chen C, Jin D, Ouyang X, Zhao L, Qiu X, Wang F (2018) Effect of structural characteristics on the depolymerization of lignin into phenolic monomers. Fuel 223:366–372
21. Jiang Z, Hu C (2016) Selective extraction and conversion of lignin in actual biomass to monophenols: a review. J Energy Chem 25(6):947–956
22. Si Z, Zhang X, Wang C, Ma L, Dong R (2017) An overview on catalytic hydrodeoxygenation of pyrolysis oil and its model compounds. Catalysts 7(6):169
23. Yang Y, Lv G, Deng L, Lu B, Li J, Zhang J et al (2017) Renewable aromatic production through hydrodeoxygenation of model bio-oil over mesoporous Ni/SBA-15 and Co/SBA-15. Microporous Mesoporous Mater 250:47–54
24. Simakova IL, Murzin DY (2016) Transformation of bio-derived acids into fuel-like alkanes via ketonic decarboxylation and hydrodeoxygenation: design of multifunctional catalyst, kinetic and mechanistic aspects. J Energy Chem 25(2):208–224
25. Abhari R, Tomlinson L, Havlik P, Jannasch N (2010) Process for co-producing jet fuel and LPG from renewable sources. Google Patents
26. Saidi M, Jahangiri A (2017) Refinery approach of bio-oils derived from fast pyrolysis of lignin to jet fuel range hydrocarbons: reaction network development for catalytic conversion of cyclohexanone. Chem Eng Res Des 121:393–406
27. Nakagawa Y, Tamura M, Tomishige K (2019) Recent development of production technology of diesel-and jet-fuel-range hydrocarbons from inedible biomass. Fuel Process Technol 193:404–422
28. Mosallanejad A, Taghvaei H, Mirsoleimani-azizi SM, Mohammadi A, Rahimpour MR (2017) Plasma upgrading of 4methylanisole: a novel approach for hydrodeoxygenation of bio oil without using a hydrogen source. Chem Eng Res Des 121:113–124
29. Karkevandi FS, Bakhtyari A, Rahimpour MR, Keshavarz P (2019) Isothermal vapor-liquid equilibrium of binary and ternary systems of anisole, hexane, and toluene and ternary system of methyl tert-butyl ether, hexane, and toluene. Thermochim Acta 682:178413
30. Gamliel DP, Baillie BP, Augustine E, Hall J, Bollas GM, Valla JA (2018) Nickel impregnated mesoporous USY zeolites for hydrodeoxygenation of anisole. Microporous Mesoporous Mater 261:18–28
31. Diao X, Ji N, Zheng M, Liu Q, Song C, Huang Y et al (2018) MgFe hydrotalcites-derived layered structure iron molybdenum sulfide catalysts for eugenol hydrodeoxygenation to produce phenolic chemicals. J Energy Chem 27(2):600–610
32. Wang Q, Gupta N, Wen G, Hamid SBA, Su DS (2017) Palladium and carbon synergistically catalyzed room-temperature hydrodeoxygenation (HDO) of vanillyl alcohol–A typical lignin model molecule. J Energy Chem 26(1):8–16
33. Shu R, Li R, Lin B, Wang C, Cheng Z, Chen Y (2020) A review on the catalytic hydrodeoxygenation of lignin-derived phenolic compounds and the conversion of raw lignin to hydrocarbon liquid fuels. Biomass Bioenerg 132:105432
34. Li X, Chen G, Liu C, Ma W, Yan B, Zhang J (2017) Hydrodeoxygenation of lignin-derived bio-oil using molecular sieves supported metal catalysts: a critical review. Renew Sustain Energy Rev 71:296–308
35. Zhou M, Wang Y, Wang Y, Xiao G (2015) Catalytic conversion of guaiacol to alcohols for bio-oil upgrading. J Energy Chem 24(4):425–431
36. Saidi M, Rostami P, Rahimpour MR, Gates BC, Raeissi S (2015) Upgrading of lignin-derived bio-oil components catalyzed by pt/γ-Al_2O_3: kinetics and reaction pathways characterizing conversion of cyclohexanone with H_2. Energy Fuels 29(1):191–199
37. Nimmanwudipong T, Runnebaum RC, Tay K, Block DE, Gates BC (2011) Cyclohexanone conversion catalyzed by Pt/γ-Al_2O_3: evidence of oxygen removal and coupling reactions. Catal Lett 141(8):1072
38. Runnebaum RC, Nimmanwudipong T, Block DE, Gates BC (2012) Catalytic conversion of compounds representative of lignin-derived bio-oils: a reaction network for guaiacol, anisole, 4-methylanisole, and cyclohexanone conversion catalysed by Pt/γ-Al_2O_3. Catal Sci Technol 2(1):113–118
39. Saidi M, Rostami P, Rahimpour MR, Gates BC, Raeissi S (2014) Upgrading of lignin-derived bio-oil components catalyzed by pt/γ-Al_2O_3: kinetics and reaction pathways characterizing conversion of cyclohexanone with H_2. Energy Fuels 29(1):191–199
40. Bakhtyari A, Rahimpour MR, Raeissi S (2020) Cobalt-molybdenum catalysts for the hydrodeoxygenation of cyclohexanone. Renew Energy 150:443–455
41. Bakhtyari A, Sakhayi A, Rahimpour MR, Raeissi S (2020) The utilization of synthesis gas for the deoxygenation of cyclohexanone over alumina-supported catalysts: screening catalysts. Asia-Pac J Chem Eng 15:e2425
42. Bakhtyari A, Sakhayi A, Rahimpour MR, Raeissi S (2020) Upgrading of cyclohexanone to hydrocarbons by hydrodeoxygenation over nickel–molybdenum catalysts. Int J Hydrog Energy 45:11062–11076
43. Taghvaei H, Bakhtyari A, Reza Rahimpour M (2020) Carbon nanotube supported nickel catalysts for anisole and cyclohexanone conversion in the presence of hydrogen and synthesis gas: effect of plasma, acid, and thermal functionalization. Fuel 288:119698
44. Alvarez F, Ribeiro FR, Guisnet M (1994) Transformation of cyclohexanone on PtHZSM5 catalysts—reaction scheme. J Mol Catal 92(1):67–79
45. Silva A, Alvarez F, Ribeiro FR, Guisnet M (2000) Synthesis of cyclohexylcyclohexanone on bifunctional Pd faujasites: influence of the balance between the acidity and the metallic function. Catal Today 60(3–4):311–317
46. Olivas A, Samano E, Fuentes S (2001) Hydrogenation of cyclohexanone on nickel–tungsten sulfide catalysts. Appl Catal A 220(1–2):279–285
47. Prasomsri T, Nimmanwudipong T, Román-Leshkov Y (2013) Effective hydrodeoxygenation of biomass-derived oxygenates into unsaturated hydrocarbons by MoO_3 using low H_2 pressures. Energy Environ Sci 6(6):1732–1738
48. Kong X, Lai W, Tian J, Li Y, Yan X, Chen L (2013) Efficient hydrodeoxygenation of aliphatic ketones over an alkali-treated Ni/HZSM-5 Catalyst. ChemCatChem 5(7):2009–2014
49. Du X, Kong X, Chen L (2014) Influence of binder on catalytic performance of Ni/HZSM-5 for hydrodeoxygenation of cyclohexanone. Catal Commun 45:109–113
50. Kong X, Liu J (2014) Influence of alumina binder content on catalytic performance of Ni/HZSM-5 for hydrodeoxygenation of cyclohexanone. PLoS ONE 9(7):e101744
51. Rahimpour HR, Saidi M, Rostami P, Gates BC, Rahimpour MR (2016) Experimental investigation on upgrading of lignin-derived bio-oils: kinetic analysis of anisole conversion on sulfided CoMo/Al_2O_3 catalyst. Int J Chem Kinet 48(11):702–713
52. Saidi M, Rahimpour HR, Rahzani B, Rostami P, Gates BC, Rahimpour MR (2016) Hydroprocessing of 4-methylanisole as a representative of lignin-derived bio-oils catalyzed by sulphided CoMo/γ-Al_2O_3: a semi-quantitative reaction network. Can J Chem Eng 94(8):1524–1532
53. Bui VN, Laurenti D, Afanasiev P, Geantet C (2011) Hydrodeoxygenation of guaiacol with CoMo catalysts. Part I: promoting

effect of cobalt on HDO selectivity and activity. Appl Catal B 101(3):239–45
54. Van N, Laurenti D, Delichere P, Geantet C (2011) Hydrodeoxygenation of guaiacol. Part II: support effect for CoMoS catalysts on HDO activity and selectivity. Appl Catal B 101(3–4):246–255
55. Jongerius AL, Jastrzebski R, Bruijnincx PC, Weckhuysen BM (2012) CoMo sulfide-catalyzed hydrodeoxygenation of lignin model compounds: An extended reaction network for the conversion of monomeric and dimeric substrates. J Catal 285(1):315–323
56. Zhou M, Ye J, Liu P, Xu J, Jiang J (2017) Water-assisted selective hydrodeoxygenation of guaiacol to cyclohexanol over supported Ni and Co bimetallic catalysts. ACS Sustain Chem Eng 5(10):8824–8835
57. Zhang X, Tang W, Zhang Q, Wang T, Ma L (2018) Hydrodeoxygenation of lignin-derived phenoic compounds to hydrocarbon fuel over supported Ni-based catalysts. Appl Energy 227:73–79
58. Gonšalves VO, Brunet S, Richard F (2016) Hydrodeoxygenation of cresols over Mo/Al_2O_3 and $CoMo/Al_2O_3$ sulfided catalysts. Catal Lett 146(8):1562–1573
59. Wang H, Feng M, Yang B (2017) Catalytic hydrodeoxygenation of anisole: an insight into the role of metals in transalkylation reactions in bio-oil upgrading. Green Chem 19(7):1668–1673
60. He Z, Wang X (2014) Highly selective catalytic hydrodeoxygenation of guaiacol to cyclohexane over Pt/TiO_2 and $NiMo/Al_2O_3$ catalysts. Front Chem Sci Eng 8(3):369–377
61. Rahzani B, Saidi M, Rahimpour HR, Gates BC, Rahimpour MR (2017) Experimental investigation of upgrading of lignin-derived bio-oil component anisole catalyzed by carbon nanotube-supported molybdenum. RSC Adv 7(17):10545–10556
62. Saidi M, Rahimpour MR, Raeissi S (2015) Upgrading process of 4-methylanisole as a lignin-derived bio-oil catalyzed by Pt/γ-Al_2O_3: kinetic investigation and reaction network development. Energy Fuels 29(5):3335–3344
63. Saidi M, Rahzani B, Rahimpour MR (2017) Characterization and catalytic properties of molybdenum supported on nano gamma Al_2O_3 for upgrading of anisole model compound. Chem Eng J 319:143–154
64. Saidi M, Rostami P, Rahimpour HR, Roshanfekr Fallah MA, Rahimpour MR, Gates BC et al (2015) Kinetics of upgrading of anisole with hydrogen catalyzed by platinum supported on alumina. Energy Fuels 29(8):4990–4997
65. Taghvaei H, Rahimpour MR, Bruggeman P (2017) Catalytic hydrodeoxygenation of anisole over nickel supported on plasma treated alumina–silica mixed oxides. RSC Adv 7(49):30990–30998
66. Zhao C, He J, Lemonidou AA, Li X, Lercher JA (2011) Aqueous-phase hydrodeoxygenation of bio-derived phenols to cycloalkanes. J Catal 280(1):8–16
67. Huynh TM, Armbruster U, Nguyen LH, Nguyen DA, Martin A (2015) Hydrodeoxygenation of bio-oil on bimetallic catalysts: from model compound to real feed. J Sustain Bioenergy Syst 5(04):151
68. Wu S-K, Lai P-C, Lin Y-C (2014) Atmospheric hydrodeoxygenation of guaiacol over nickel phosphide catalysts: effect of phosphorus composition. Catal Lett 144(5):878–889
69. Wu S-K, Lai P-C, Lin Y-C, Wan H-P, Lee H-T, Chang Y-H (2013) Atmospheric hydrodeoxygenation of guaiacol over alumina-, zirconia-, and silica-supported nickel phosphide catalysts. ACS Sustain Chem Eng 1(3):349–358
70. Shu R, Xu Y, Ma L, Zhang Q, Chen P, Wang T (2017) Synergistic effects of highly active Ni and acid site on the hydrodeoxygenation of syringol. Catal Commun 91:1–5
71. Demirbas A (2007) Effects of moisture and hydrogen content on the heating value of fuels. Energy Sour Part A 29(7):649–655
72. Milne T, Brennan A, Glenn BH (1990) Sourcebook of methods of analysis for biomass and biomass conversion processes. Springer, New York
73. Li X, Chai Y, Liu B, Liu H, Li J, Zhao R et al (2014) Hydrodesulfurization of 4,6-dimethyldibenzothiophene over CoMo catalysts supported on γ-alumina with different morphology. Ind Eng Chem Res 53(23):9665–9673
74. Van Veen JR, Gerkema E, van der Kraan AM, Hendriks PA, Beens H (1992) A 57Co Mössbauer emission spectrometric study of some supported CoMo hydrodesulfurization catalysts. J Catal 133(1):112–123
75. Jiang M, Wang B, Yao Y, Li Z, Ma X, Qin S et al (2013) Effect of sulfidation temperature on $CoO–MoO_3/\gamma$-Al_2O_3 catalyst for sulfur-resistant methanation. Catal Sci Technol 3(10):2793–2800
76. Ibrahim AA, Lin A, Zhang F, AbouZeid KM, El-Shall MS (2017) Palladium nanoparticles supported on a metal-organic framework-partially reduced graphene oxide hybrid for the catalytic hydrodeoxygenation of vanillin as a model for biofuel upgrade reactions. ChemCatChem 9(3):469–480
77. Saih Y, Nagata M, Funamoto T, Masuyama Y, Segawa K (2005) Ultra deep hydrodesulfurization of dibenzothiophene derivatives over $NiMo/TiO_2$-Al_2O_3 catalysts. Appl Catal A 295(1):11–22
78. Behnejad B, Abdouss M, Tavasoli A (2019) Comparison of performance of Ni–Mo/γ-alumina catalyst in HDS and HDN reactions of main distillate fractions. Pet Sci 16:645–656
79. Yi X, Guo D, Li P, Lian X, Xu Y, Dong Y et al (2017) One pot synthesis of $NiMo–Al_2O_3$ catalysts by solvent-free solid-state method for hydrodesulfurization. RSC Adv 7(86):54468–54474
80. Kaluža L, Palcheva R, Spojakina A, Jirátová K, Tyuliev G (2012) Hydrodesulfurization NiMo catalysts supported on Co, Ni and B modified Al_2O_3 from Anderson heteropolymolybdates. Procedia Eng 42:873–884
81. Zhang M-h, Fan J-y, Chi K, Duan A-j, Zhao Z, Meng X-l et al (2017) Synthesis, characterization, and catalytic performance of NiMo catalysts supported on different crystal alumina materials in the hydrodesulfurization of diesel. Fuel Processing Technology 156:446–53
82. Chen W, Maugé F, van Gestel J, Nie H, Li D, Long X (2013) Effect of modification of the alumina acidity on the properties of supported Mo and CoMo sulfide catalysts. J Catal 304:47–62
83. Høj M, Linde K, Hansen TK, Brorson M, Jensen AD, Grunwaldt J-D (2011) Flame spray synthesis of $CoMo/Al_2O_3$ hydrotreating catalysts. Appl Catal A 397(1–2):201–208
84. Cordero RL, Llambias FG, Agudo AL (1991) Temperature-programmed reduction and zeta potential studies of the structure of$Mo/O_3Al_2O_3$ andMo/O_3SiO_2 catalysts effect of the impregnation pH and molybdenum loading. Appl Catal 74(1):125–136
85. Arnoldy P, Franken M, Scheffer B, Moulijn J (1985) Temperature-programmed reduction of CoO $MoO_3Al_2O_3$ catalysts. J Catal 96(2):381–395
86. González-Cortés SL, Xiao T-C, Lin T-W, Green ML (2006) Influence of double promotion on HDS catalysts prepared by urea-matrix combustion synthesis. Appl Catal A 302(2):264–273
87. Cordero RL, Agudo AL (2000) Effect of water extraction on the surface properties of Mo/Al_2O_3 and $NiMo/Al_2O_3$ hydrotreating catalysts. Appl Catal A 202(1):23–35
88. Rynkowski J, Paryjczak T, Lenik M (1993) On the nature of oxidic nickel phases in NiO/γ-Al_2O_3 catalysts. Appl Catal A 106(1):73–82
89. Scheffer B, Molhoek P, Moulijn J (1989) Temperature-programmed reduction of $NiOWO_3/Al_2O_3$ hydrodesulphurization catalysts. Appl Catal 46(1):11–30
90. Brito JL, Laine J (1993) Reducibility of $Ni-Mo/Al_2O_3$ catalysts: a TPR study. J Catal 139(2):540–550

91. Arena F, Dario R, Parmaliana A (1998) A characterization study of the surface acidity of solid catalysts by temperature programmed methods. Appl Catal A 170(1):127–137
92. Damyanova S, Spojakina A, Jiratova K (1995) Effect of mixed titania-alumina supports on the phase composition of NiMo/$TiO_2Al_2O_3$ catalysts. Appl Catal A 125(2):257–269
93. Laine J, Brito J, Severino F (1985) Carbon deposition and hydrodesulfurization activity of nickel-molybdenum supported catalysts. Appl Catal 15(2):333–338
94. Sing KS (1985) Reporting physisorption data for gas/solid systems with special reference to the determination of surface area and porosity (Recommendations 1984). Pure Appl Chem 57(4):603–619
95. Campbell ML (2000) Cyclohexane. In: Gerhartz W (ed) Ullmann's encyclopedia of industrial chemistry. Wiley, Weinheim
96. Triwahyono S, Jalil AA, Hamdan H (2006) Isomerisation of cyclohexane to methylcyclopentane over Pt/SO_4 2–ZrO_2 Catalyst. J Inst Eng Malays 67(1):30–35
97. Wrzyszcz J, Zawadzki M, Trawczyński J, Grabowska H, Mišta W (2001) Some catalytic properties of hydrothermally synthesised zinc aluminate spinel. Appl Catal A 210(1):263–269
98. Aboul-Gheit AK, Aboul-Fotouh SM, Aboul-Gheit NAK (2005) Hydroconversion of cyclohexene using catalysts containing Pt, Pd, Ir and Re supported on H-ZSM-5 zeolite. Appl Catal A 283(1):157–164
99. Aboul-Gheit AK, Aboul-Gheit NAK (2006) Iridium/H-ZSM-5 zeolite catalyst promoted via hydrochlorination or hydrofluorination for the hydroconversion of cyclohexene. Appl Catal A 303(2):141–151
100. Onyestyák G, Pál-Borbély G, Beyer HK (2002) Cyclohexane conversion over H-zeolite supported platinum. Appl Catal A 229(1):65–74
101. Akhmedov VM, Al-Khowaiter SH (2000) Hydroconversion of hydrocarbons over Ru-containing supported catalysts prepared by metal vapor method. Appl Catal A 197(2):201–212
102. Campbell M (2011) Cyclohexane. In: Chadwick SS (ed) Ullmann's encyclopedia of industrial chemistry. Wiley, Weinheim
103. Folkins HO (2000) Benzene. In: Chadwick SS (ed) Ullmann's encyclopedia of industrial chemistry. Wiley, Weinheim
104. Musser MT (2000) Cyclohexanol and cyclohexanone. In: Chadwick SS (ed) Ullmann's encyclopedia of industrial chemistry. Wiley, Weinheim
105. Weber M, Weber M, Kleine-Boymann M (2004) Phenol. In: Chadwick SS (ed) Ullmann's encyclopedia of industrial chemistry. Wiley, Weinheim
106. Plotkin JS (2016) What's new in phenol production. American Chemical Society https://www.acs.org/content/acs/en/pressroom/cutting-edge-chemistry/what-s-new-in-phenol-production-.html. Accessed 10 May 2018

Authors and Affiliations

Ali Bakhtyari[1] · Adele Sakhayi[1] · Zohre Moravvej[1] · Mohammad Reza Rahimpour[1]

✉ Mohammad Reza Rahimpour
rahimpor@shirazu.ac.ir

[1] Department of Chemical Engineering, Shiraz University, 71345 Shiraz, Iran